Available online at www.sciencedirect.com
ScienceDirect

Journal of the Mechanics and Physics of Solids 56 (2008) 772–800

JOURNAL OF THE MECHANICS AND PHYSICS OF SOLIDS

www.elsevier.com/locate/jmps

On boundary potential energies in deformational and configurational mechanics

Paul Steinmann

Chair of Applied Mechanics, University of Kaiserslautern, D-67653 Kaiserslautern, Germany

Received 11 April 2007; received in revised form 29 June 2007; accepted 3 July 2007

Abstract

This contribution deals with the implications of boundary potential energies, i.e. in short *surface, curve* and *point* potentials, on deformational and configurational mechanics. Within the realm of deformational mechanics the surface/curve potentials are allowed in the most general case to depend on the deformation, the surface/curve deformation gradient and the spatial surface normal/curve tangent and are parametrised in the material placement and the material surface normal/curve tangent. The point potentials depend on the deformation and are parametrised in the material placement. From the configurational mechanics perspective the roles of fields and parametrisations are reversed. By considering variational arguments based on the kinematics of deforming surfaces/curves, in particular the relevant surface/curve stresses and distributed forces contributing to (localized) deformational and configurational force balances at surfaces/curves/points, which extend the common traction boundary conditions, are derived. Thereby, dissipative distributed configurational forces that are energetically conjugate to configurational changes are introduced as definitions. The (localized) force balances at surfaces/curves/points together with the contributing stresses and distributed forces within deformational and configurational mechanics display an intriguing duality. The resulting dissipative configurational tractions at the boundary are exemplified for some illustrative cases of boundary potentials.

Keywords: Boundary energies; Surface/curve tension and stress; Configurational mechanics

1. Introduction

Configurational mechanics is concerned with changes of the material configuration of continuum bodies, i.e. with configurational changes. Thereby, configurational changes are due to the kinetics of all kind of defects like e.g. vacancies or inclusions, cracks, interfaces or phase boundaries and the like. The defect kinetics are in turn due to so-called configurational forces.[1] All the above cases can essentially be treated by considering the configurational changes at boundaries to continuum bodies or to their subparts (recall e.g. the cut-out and

E-mail address: ps@rhrk.uni-kl.de

[1]A descriptive definition of configurational forces is given in the seminal work by Eshelby (1951): *…the total energy of a system… is a function of the set of parameters necessary to specify the configuration of the imperfections. The negative gradient of the total energy wrt the position of an imperfection may conveniently be called the force on it. This force, in a sense fictitious, is introduced to give a picturesque description of energy changes, and must not be confused with the ordinary surface and body forces acting on the material.*

0022-5096/$ - see front matter
doi:10.1016/j.jmps.2007.07.001

limiting procedure in the definition of the classical J-integral). Configurational mechanics has been a very active field recently: comprehensive overviews that discuss various aspects of configurational mechanics can be found e.g. in Maugin (1993,1995), Gurtin (1995,2000) or Kienzler and Herrmann (2000), own contributions to the field are, e.g. Steinmann (2002a–c).

The aim of this particular contribution is to variationally derive the (localized) force balances at surfaces/curves/points and the associated stresses and forces at boundaries within configurational mechanics. Thereby in particular effects of boundary potential energies are taken into account. By doing so, the intriguing duality of deformational and configurational mechanics is revealed as a by-product.

The motivation for this work, i.e. to consider boundary potential energies, are essentially the following observations:

(i) Inspired by an atomistic/molecular picture of materials, which is of particular relevance in the realm of nanomechanics, it is obvious that the boundary of a continuum body (or an interface between subparts of a continuum body) displays different properties as compared to its bulk. This phenomenon is usually modelled in terms of surface/curve tension. The notion of a scalar valued surface/curve tension can be generalised to a surface/curve stress of tensorial nature, see e.g. Gurtin and Murdoch (1975). For a conservative case the surface/curve stress derives from a boundary potential that depends on the so-called surface/curve deformation gradient quite like in the case of elastic membranes/strings. In addition, the boundary potential might depend on the surface normal/curve tangent if anisotropies have to be captured. Typical applications of boundary free energy are in the area of nanomechanics, see e.g. Dingreville et al. (2005) and references therein. The effect of surface/curve stress within configurational mechanics is thus in particular of interest when it comes to the assesment of defects at the nanoscale.

(ii) Moreover, in materials processing, the boundary of materials is frequently exposed to, e.g., oxidation, ageing, grit blasting, plasma jet treatment, etc., thus obviously resulting in distinctively different properties in comparatively thin boundary layers. Likewise, coating materials with thin films results clearly in different properties at the boundary. These effects could phenomenologically be modelled in terms of boundaries equipped with their own potential energy (free energy in a thermomechanical setting).

(iii) Finally, boundary tractions are frequently assumed to be conservative, thus in this case they can be derived from a boundary potential energy that depends on the deformation. Clearly, in order to realistically describe the possibilities for mechanical loading of a continuum body, boundary tractions are of eminent importance. Nevertheless, since the consideration of boundary potentials or boundary traction within a configurational mechanics setting poses severe difficulties due to the need to consider the geometry and kinematics of configurational changes of the boundary, boundary potentials are often simply not considered in this context. Thus the application of configurational mechanics to realistic problems is often somewhat restricted if boundary tractions cannot routinely be taken into account.

As a conclusion, the case of boundary traction and surface/curve stress (as a tensorial generalisation of surface/curve tension) with possible dependence on the surface normal/curve tangent shall be treated within the same framework. Thus, within deformational mechanics, in addition to potentials in the bulk, boundary potentials depending in the most general case on the deformation, the surface/curve deformation gradient and the spatial surface normal/curve tangent with possible parametrisation in the material placement and the material surface normal/curve tangent have to be considered. Then, for the case of configurational mechanics the role of fields and parametrisation will simply be reversed. This will be the basic set up for the subsequent developments in this contribution.

The thermomechanics of configurational (material in the terminology of Maugin) forces acting on singular surfaces or rather discontinuities have already been considered, e.g., in the early contribution of Abeyaratne and Knowles (1990) and in a series of publications by Maugin and Trimarco (1995) and Maugin (1997,1998a, b,1999). Nevertheless, there the effects of surface/curve stress are not taken into account.

A first comprehensive, purely mechanical approach towards the treatment of elastic material surfaces was proposed by Gurtin and Murdoch (1975). Here, besides providing all the necessary results for the kinematics and balance laws for surfaces, in particular the tensorial nature of surface tension within deformational mechanics was established. This approach was subsequently extended in a series of contributions by Gurtin (1988), Angenent and Gurtin (1989) and Gurtin and Struthers (1990) towards the thermomechanics of interfaces. In this line of developments, motivated by the milestone contribution by Leo and Sekerka (1989), the incorporation of configurational (accretive in the early terminology of Gurtin) forces in addition to deformational forces was considered by Gurtin and Struthers (1990) and Gurtin (1993). Contributions almost entirely devoted to the configurational mechanics of interfaces are by (Gurtin (1995,2000), which derive the relevant surface balance equations essentially from non-standard (material) observer invariance. Similar results within the framework of multifield theories have been derived along the same lines e.g. by Mariano (2000,2002).

The extension to junctions of interfaces in a two- and three-dimensional setting was initially proposed by Simha and Bhattacharya (1998,2000). Here the curve defining the junction of several interfaces is equipped with its own thermomechanical ingredients. Applications of these modelling concepts to junctions within the setting of materials with substructure have been contributed by Mariano (2001), Capriz and Mariano (2004).

The philosophy of this contribution is somewhat different from the above references: within a variational (hyperelastic) framework configurational forces are *defined* as capturing energetic changes that go along with so-called material variations, i.e. configurational changes. Thus the energy release or rather the dissipation resulting from material variations, i.e. variations at fixed spatial placements, is considered. For a conservative problem material variations of the total potential energy functional render, unlike the ordinary spatial variations, i.e. variations at fixed material placements, non-zero changes of the total potential energy. These changes have to respect the second law, thus the energy released (the dissipation) has to be negative (positive). Non-zero changes of the total potential energy as a result of material variations characterise the absence of so-called configurational equilibrium. The non-equilibrium or rather dissipative part of the configurational force system acts as the driving force for the kinetics of all kinds of defects, i.e. configurational changes. Vice versa, for the case of configurational equilibrium there is absolutely no tendency for configurational changes.

A main thrust of this contribution is to emphasize the striking duality of (but also the difference between) the (localized) force balances at surfaces/curves/points within deformational and configurational mechanics, whereby especially boundary potentials are taken into account. Here it deserves mentioning that the relevant curve quantities are formulated, quite like in the cases of surfaces and bulk, in a tensor rather than the common vector representation. Moreover it appears that point potentials have not been considered in the present context elsewhere. It turns out that for perfect, i.e. defect free surfaces/curves the tangential part of the (localized) force balance at surfaces/curves can be cast into four different formats by performing either surface/curve Piola transformations or surface/curve pull back/push forward operations, a result resembling known relations in the bulk, see e.g. Maugin and Trimarco (1992) or Maugin (1993). In particular, with the present developments the necessary prerequisites are provided to take into account ordinary boundary tractions (which are often neglected in treatises on configurational forces), within configurational mechanics.

The manuscript is organised as follows: Section 2 reiterates briefly, as a preparation for the subsequent developments, some essential results pertaining to the geometry on surfaces and curves. Section 3 is concerned with the kinematics of a continuum body, whereby the focus is essentially on the kinematics of its deforming boundary surfaces and curves. Here a number of important results like e.g. the surface area/curve line maps, the surface/curve Nanson formula, the surface/curve Piola identity and the surface/curve Piola transforms are derived. Section 4 deals with the treatment of boundary potentials within deformational mechanics. Thereby the relevant balance equations are derived from a variational viewpoint in terms of two-point (Piola) and spatial description (Cauchy) stresses. Section 5 develops the relevant balance equations within configurational mechanics, whereby again two-point and material description (Eshelby) stresses are considered. Here distributed configurational forces are defined as capturing the energetic changes that go along with configurational changes. The section closes with highlighting the intriguing duality of the deformational and the configurational settings and concludes with four different formats for the tangential part of the (localized) force balance at surfaces/curves. Section 6 exemplifies the previous developments for some illustrative cases of boundary potentials. Sections 7 finally concludes the manuscript.

The main notation is assembled for the convenience of the reader in Table 1.

2. Geometry on surfaces and curves

To set the stage, first some basic notations, terminologies and results for the geometry on surfaces and curves, that are needed in the sequel, are briefly reviewed.

Table 1
Notation used to denote operators and quantities in the bulk, at surfaces, at curves and at points: upper/lower case letters or the indices $0, t$, respectively, refer to the material/spatial configuration

	Bulk	Surfaces	Curves	Points
Counter	–	ς	κ	π
Domain	$\mathscr{B}_{0,t}$	$\mathscr{S}_{0,t}$	$\mathscr{C}_{0,t}$	$\mathscr{P}_{0,t}$
Gradient	$\mathrm{Grad}\{\bullet\}, \mathrm{grad}\{\bullet\}$	$\widehat{\mathrm{Grad}}\{\bullet\}, \widehat{\mathrm{grad}}\{\bullet\}$	$\widetilde{\mathrm{Grad}}\{\bullet\}, \widetilde{\mathrm{grad}}\{\bullet\}$	–
Divergence	$\mathrm{Div}\{\bullet\}, \mathrm{div}\{\bullet\}$	$\widehat{\mathrm{Div}}\{\bullet\}, \widehat{\mathrm{div}}\{\bullet\}$	$\widetilde{\mathrm{Div}}\{\bullet\}, \widetilde{\mathrm{div}}\{\bullet\}$	–
Tangent	–	$\boldsymbol{A}_\alpha, \boldsymbol{a}_\alpha$	$\boldsymbol{T}, \boldsymbol{t}$	–
Normal/Binormal	–	$\boldsymbol{N}, \boldsymbol{n}$	$\boldsymbol{M}, \boldsymbol{B}, \boldsymbol{m}, \boldsymbol{b}$	–
Boundary normal	$\boldsymbol{N}, \boldsymbol{n}$	$\widehat{\boldsymbol{N}}, \widehat{\boldsymbol{n}}$	$\widetilde{\boldsymbol{M}}, \widetilde{\boldsymbol{m}}$	–
Differential element	$\mathrm{d}V$, $\mathrm{d}v$	$\mathrm{d}A$, $\mathrm{d}a$	$\mathrm{d}L$, $\mathrm{d}l$	1
Oriented element	–	$\mathrm{d}\boldsymbol{A}$, $\mathrm{d}\boldsymbol{a}$	$\mathrm{d}\widehat{\boldsymbol{L}}$, $\mathrm{d}\widehat{\boldsymbol{l}}$	$\widetilde{\boldsymbol{M}}, \widetilde{\boldsymbol{m}}$
Unit tensor	$\boldsymbol{I}, \boldsymbol{i}$	$\widehat{\boldsymbol{I}}, \widehat{\boldsymbol{i}}$	$\widetilde{\boldsymbol{I}}, \widetilde{\boldsymbol{I}}^{\perp}, \widetilde{\boldsymbol{i}}, \widetilde{\boldsymbol{i}}^{\perp}$	–
Curvature	–	$K, \boldsymbol{K}, k, \boldsymbol{k}$	$\mathsf{C}, \boldsymbol{C}_\parallel, \boldsymbol{C}_\perp, \mathsf{c}, \boldsymbol{c}_\parallel, \boldsymbol{c}_\perp$	–
Deformation map	$\boldsymbol{\varphi}, \boldsymbol{\Phi}$	$\boldsymbol{\varphi}, \boldsymbol{\Phi}$	$\boldsymbol{\varphi}, \boldsymbol{\Phi}$	$\boldsymbol{\varphi}, \boldsymbol{\Phi}$
Tangent map	$\boldsymbol{F}, \boldsymbol{f}$	$\widehat{\boldsymbol{F}}, \widehat{\boldsymbol{f}}$	$\widetilde{\boldsymbol{F}}, \widetilde{\boldsymbol{f}}$	–
Area map	$\mathrm{cof}\,\boldsymbol{F}, \mathrm{cof}\,\boldsymbol{f}$	$\widehat{\mathrm{cof}\,\boldsymbol{F}}, \widehat{\mathrm{cof}\,\boldsymbol{f}}$	$\widetilde{\mathrm{cof}\,\boldsymbol{F}}, \widetilde{\mathrm{cof}\,\boldsymbol{f}}$	–
Volume map	J, j	$\widehat{J}, \widehat{j}$	$\widetilde{J}, \widetilde{j}$	–
Energy density	$U_{0,t}, W_{0,t}, V_{0,t}$	$u_{0,t}, w_{0,t}, v_{0,t}$	$\mathsf{u}_{0,t}, \mathsf{w}_{0,t}, \mathsf{v}_{0,t}$	u
Deformational				
Piola stress	$\boldsymbol{P}$	$\widehat{\boldsymbol{P}}$	$\widetilde{\boldsymbol{P}}$	–
Cauchy stress	$\boldsymbol{\sigma}$	$\widehat{\boldsymbol{\sigma}}$	$\widetilde{\boldsymbol{\sigma}}$	–
Force density	$\boldsymbol{b}_{0,t}$	$\widehat{\boldsymbol{b}}_{0,t}$	$\widetilde{\boldsymbol{b}}_{0,t}$	$\bar{\boldsymbol{b}}$
Shear		$\widehat{\boldsymbol{S}}_{0,t}, \widehat{\boldsymbol{\pi}}_{0,t}$	$\widetilde{\boldsymbol{\pi}}_{0,t}$	–
Configurational				
Piola stress	$\boldsymbol{p}$	$\widehat{\boldsymbol{p}}$	$\widetilde{\boldsymbol{p}}$	–
Cauchy stress	$\boldsymbol{\Sigma}$	$\widehat{\boldsymbol{\Sigma}}$	$\widetilde{\boldsymbol{\Sigma}}$	–
Force density	$\boldsymbol{B}_{0,t}$	$\widehat{\boldsymbol{B}}_{0,t}$	$\widetilde{\boldsymbol{B}}_{0,t}$	$\bar{\boldsymbol{B}}$
Shear		$\widehat{\boldsymbol{s}}_{0,t}, \widehat{\boldsymbol{\Pi}}_{0,t}$	$\widetilde{\boldsymbol{\Pi}}_{0,t}$	–

2.1. Surfaces

A two-dimensional (smooth) surface $\mathscr{S}$ in the three-dimensional, embedding euclidian space with coordinates $\boldsymbol{x}$ is parametrised by two surface coordinates θ^α with $\alpha = 1, 2$ as

$$\boldsymbol{x} = \boldsymbol{x}(\theta^\alpha). \tag{1}$$

The corresponding tangent vectors $\boldsymbol{a}_\alpha \in T\mathscr{S}$ to the surface coordinate lines θ^α, i.e. the covariant (natural) surface basis vectors are given by

$$\boldsymbol{a}_\alpha = \partial_{\theta^\alpha}\boldsymbol{x}. \tag{2}$$

The associated contravariant (dual) surface basis vectors $\boldsymbol{a}^\alpha$ are defined by the Kronecker property $\delta^\alpha{}_\beta = \boldsymbol{a}^\alpha \cdot \boldsymbol{a}_\beta$ and are explicitly related to the covariant surface basis vectors $\boldsymbol{a}_\alpha$ by the co- and contravariant surface metric coefficients $a_{\alpha\beta}$ (first fundamental form for the surface) and $a^{\alpha\beta}$, respectively, as

$$\boldsymbol{a}_\alpha = a_{\alpha\beta}\boldsymbol{a}^\beta \quad \text{with } a_{\alpha\beta} = \boldsymbol{a}_\alpha \cdot \boldsymbol{a}_\beta = [a^{\alpha\beta}]^{-1}, \tag{3}$$

$$\boldsymbol{a}^\alpha = a^{\alpha\beta}\boldsymbol{a}_\beta \quad \text{with } a^{\alpha\beta} = \boldsymbol{a}^\alpha \cdot \boldsymbol{a}^\beta = [a_{\alpha\beta}]^{-1}.$$

The contra- and covariant base vectors $\boldsymbol{a}^3$ and $\boldsymbol{a}_3$, normal to $T\mathscr{S}$, are defined by

$$\boldsymbol{a}^3 := \boldsymbol{a}_1 \times \boldsymbol{a}_2 \quad \text{and} \quad \boldsymbol{a}_3 := [a^{33}]^{-1}\boldsymbol{a}^3 \quad \text{so that } \boldsymbol{a}^3 \cdot \boldsymbol{a}_3 = 1. \tag{4}$$

Thereby, the corresponding contra- and covariant metric coefficients a^{33} and a_{33} follow as

$$a^{33} = |\boldsymbol{a}_1 \times \boldsymbol{a}_2|^2 = \det[a_{\alpha\beta}] = [\det[a^{\alpha\beta}]]^{-1} = [a_{33}]^{-1}. \tag{5}$$

Accordingly, the surface area element $\mathrm{d}a$ and the surface normal $\boldsymbol{n}$ are computed as

$$\mathrm{d}a = |\boldsymbol{a}_1 \times \boldsymbol{a}_2|\,\mathrm{d}\theta^1\,\mathrm{d}\theta^2 = [a^{33}]^{1/2}\,\mathrm{d}\theta^1\,\mathrm{d}\theta^2 \quad \text{and} \quad \boldsymbol{n} = [a_{33}]^{1/2}\boldsymbol{a}^3 = [a^{33}]^{1/2}\boldsymbol{a}_3. \tag{6}$$

Moreover, with $\boldsymbol{i}$ the ordinary mixed-variant unit tensor of the three-dimensional, embedding euclidian space, we define the mixed-variant surface unit tensor $\widehat{\boldsymbol{i}}$ as

$$\widehat{\boldsymbol{i}} := \delta^{\alpha}{}_{\beta}\boldsymbol{a}_{\alpha} \otimes \boldsymbol{a}^{\beta} = \boldsymbol{a}_{\alpha} \otimes \boldsymbol{a}^{\alpha} = \boldsymbol{i} - \boldsymbol{a}_3 \otimes \boldsymbol{a}^3 = \boldsymbol{i} - \boldsymbol{n} \otimes \boldsymbol{n}. \tag{7}$$

Clearly the mixed-variant surface unit tensor acts as a surface (idempotent) projection tensor. Finally, the surface gradient and surface divergence operators for vector fields are defined by

$$\widehat{\mathrm{grad}}\{\bullet\} := \partial_{\theta^{\alpha}}\{\bullet\} \otimes \boldsymbol{a}^{\alpha} \quad \text{and} \quad \widehat{\mathrm{div}}\{\bullet\} := \partial_{\theta^{\alpha}}\{\bullet\} \cdot \boldsymbol{a}^{\alpha}. \tag{8}$$

As a consequence, observe that $\widehat{\mathrm{grad}}\{\bullet\} \cdot \boldsymbol{n} = \boldsymbol{0}$ holds by definition. The surface gradient and surface divergence for tensor valued fields follows from multiplying the tensor valued field $\{\bullet\}$ in Eq. (8) by an arbitrary constant vector.

Remark. Recall the Gauss formulae for the derivatives of the co- and contravariant surface basis vectors

$$\partial_{\theta^{\beta}}\boldsymbol{a}_{\alpha} = \Gamma^{\gamma}_{\alpha\beta}\boldsymbol{a}_{\gamma} + k_{\alpha\beta}\boldsymbol{n} \quad \text{and} \quad \partial_{\theta^{\beta}}\boldsymbol{a}^{\alpha} = -\Gamma^{\alpha}_{\beta\gamma}\boldsymbol{a}^{\gamma} + k^{\alpha}{}_{\beta}\boldsymbol{n}. \tag{9}$$

Here $\Gamma^{\gamma}_{\alpha\beta} = \partial_{\theta^{\beta}}\boldsymbol{a}_{\alpha} \cdot \boldsymbol{a}^{\gamma}$ denote the surface Christoffel symbols, $k_{\alpha\beta}$ are the coefficients of the curvature tensor, see below.

Example. The curvature tensor $\boldsymbol{k} = k_{\alpha\beta}\boldsymbol{a}^{\alpha} \otimes \boldsymbol{a}^{\beta}$ and the total curvature $k = k^{\alpha}_{\alpha} = k^{\alpha}_{\alpha}$ (twice the mean curvature) of the surface $\mathscr{S}$ are defined as the negative surface gradient and surface divergence of the surface normal $\boldsymbol{n}$, respectively,

$$\boldsymbol{k} := -\widehat{\mathrm{grad}}\,\boldsymbol{n} = -\partial_{\theta^{\beta}}\boldsymbol{n} \otimes \boldsymbol{a}^{\beta} \quad \text{and} \quad k := -\widehat{\mathrm{div}}\,\boldsymbol{n} = -\partial_{\theta^{\beta}}\boldsymbol{n} \cdot \boldsymbol{a}^{\beta}. \tag{10}$$

Accordingly, the surface divergence of the surface unit tensor $\widehat{\boldsymbol{i}}$ renders

$$\widehat{\mathrm{div}}\,\widehat{\boldsymbol{i}} = k\boldsymbol{n}. \tag{11}$$

The covariant coefficients of the curvature tensor (second fundamental form for the surface) are computed by $k_{\alpha\beta} = \boldsymbol{a}_{\alpha} \cdot \boldsymbol{k} \cdot \boldsymbol{a}_{\beta} = -\boldsymbol{a}_{\alpha} \cdot \partial_{\theta^{\beta}}\boldsymbol{n}$.

With the above terminology and notation we finally recall the:

Surface Divergence Theorem. *Let $\mathscr{S}'$ denote a subsurface of $\mathscr{S}$. The outward normal to the boundary curve $\mathscr{C}' := \partial\mathscr{S}'$ of the subsurface $\mathscr{S}'$, living in the cotangent space to $\mathscr{S}'$, is denoted by $\widehat{\boldsymbol{n}}$. Then the surface divergence theorem for vector valued fields $\{\bullet\}$ reads*

$$\int_{\mathscr{S}'} \widehat{\mathrm{div}}\{\bullet\}\,\mathrm{d}a = \int_{\mathscr{C}'} \{\bullet\} \cdot \widehat{\boldsymbol{n}}\,\mathrm{d}l - \int_{\mathscr{S}'} k\,\{\bullet\} \cdot \boldsymbol{n}\,\mathrm{d}a. \tag{12}$$

(*To verify the surface divergence theorem* 12 *for tensor valued fields* $\{\bullet\}$ *multiply the tensor valued field* $\{\bullet\}$ *in* 12 *by an arbitrary constant vector.*) *The surface divergence theorem is the specialisation of the ordinary Gauss theorem to surfaces. Especially if the vector field is tangent, i.e.* $\{\bullet\} \cdot \boldsymbol{n} = 0$, *the similarity is obvious.*

Moreover, as a corollary we obtain the:

Line Theorem. *Applying the surface divergence theorem to the surface unit tensor* $\widehat{\boldsymbol{i}}$ *renders the line theorem*

$$\int_{\mathscr{S}'} k\,\boldsymbol{n}\,\mathrm{d}a = \int_{\mathscr{C}'} \widehat{\boldsymbol{n}}\,\mathrm{d}l. \tag{13}$$

As an example for $\mathscr{S}'$ *consider a half sphere with* $k = 2/r$ *and axis of rotational symmetry* $\boldsymbol{e}$: *the surface integral over* $\boldsymbol{n}$ *then renders* $\pi r^2 \boldsymbol{e}$, *whereas the curve integral of* $\widehat{\boldsymbol{n}}$ *is computed as* $2\pi r\boldsymbol{e}$. *The line theorem is analogous to the well-known area theorem. Especially if* $\mathscr{S}'$ *is flat, i.e.* $k = 0$ *the similarity is obvious.*

For fields that are smooth in a three-dimensional neighbourhood $\mathscr{N}$ of the surface, the surface gradient and surface divergence operators are alternatively defined as

$$\widehat{\mathrm{grad}}\{\bullet\} := \mathrm{grad}\{\bullet\} \cdot \widehat{\boldsymbol{i}} \quad \text{and} \quad \widehat{\mathrm{div}}\{\bullet\} := \widehat{\mathrm{grad}}\{\bullet\} : \widehat{\boldsymbol{i}}. \tag{14}$$

Alternatively, a two-dimensional (smooth) surface $\mathscr{S}$ in the three-dimensional, embedding euclidian space may be defined by the zero level set $s(\boldsymbol{x}) = 0$ of a level set function $s(\boldsymbol{x})$ (which is smooth in a three-dimensional neighbourhood $\mathscr{N}$ of the surface), i.e.

$$\mathscr{S} := \{\boldsymbol{x} | s(\boldsymbol{x}) = 0\}. \tag{15}$$

The gradient of the level set function $s(\boldsymbol{x})$ at $\mathscr{S}$ then defines the surface normal $\boldsymbol{n}$

$$\boldsymbol{n} := |\mathrm{grad}\, s|^{-1} \mathrm{grad}\, s. \tag{16}$$

Example. With the above definitions for the curvature tensor $\boldsymbol{k}$ and the total curvature k of the surface $\mathscr{S}$ the alternative representations in terms of the level set function $s(\boldsymbol{x})$ are obtained

$$\boldsymbol{k} = -|\mathrm{grad}\, s|^{-1} \widehat{\boldsymbol{i}} \cdot \nabla^2_{xx} s \cdot \widehat{\boldsymbol{i}} \quad \text{and} \quad k = -|\mathrm{grad}\, s|^{-1}\ \nabla^2_{xx} s : \widehat{\boldsymbol{i}}. \tag{17}$$

Observe that the curvature tensor is symmetric and lives in the cotangent space to $\mathscr{S}$.

2.2. Curves

A one-dimensional (smooth) curve $\mathscr{C}$ in the three-dimensional, embedding euclidian space with coordinates $\boldsymbol{x}$ is parametrised by the arclength θ as

$$\boldsymbol{x} = \boldsymbol{x}(\theta). \tag{18}$$

The corresponding tangent vector $\boldsymbol{t} \in T\mathscr{C}$ to the curve, together with the (principal) normal and binormal vectors $\boldsymbol{m}$ and $\boldsymbol{b}$, orthogonal to $T\mathscr{C}$, are defined by

$$\boldsymbol{t} := \partial_\theta \boldsymbol{x} \quad \text{and} \quad \boldsymbol{m} := \partial_\theta \boldsymbol{t} / |\partial_\theta \boldsymbol{t}| \quad \text{and} \quad \boldsymbol{b} := \boldsymbol{t} \times \boldsymbol{m}. \tag{19}$$

Due to the parametrisation of the curve in its arclength θ the tangent vector $\boldsymbol{t}$ has unit length and the curve line element $\mathrm{d}l$ is computed as

$$\mathrm{d}l = |\partial_\theta \boldsymbol{x}|\,\mathrm{d}\theta = |\boldsymbol{t}|\,\mathrm{d}\theta = \mathrm{d}\theta. \tag{20}$$

Moreover, we define the mixed-variant curve unit tensor $\widetilde{\boldsymbol{i}}$ as

$$\widetilde{\boldsymbol{i}} := \boldsymbol{t} \otimes \boldsymbol{t} = \boldsymbol{i} - \boldsymbol{m} \otimes \boldsymbol{m} - \boldsymbol{b} \otimes \boldsymbol{b}. \tag{21}$$

Clearly the mixed-variant curve unit tensor acts as a curve (idempotent) projection tensor. Finally, the curve gradient and curve divergence operators for vector fields are defined by

$$\widetilde{\mathrm{grad}}\{\bullet\} := \partial_\theta\{\bullet\} \otimes \boldsymbol{t} \quad \text{and} \quad \widetilde{\mathrm{div}}\{\bullet\} := \partial_\theta\{\bullet\} \cdot \boldsymbol{t}. \tag{22}$$

As a consequence, observe that $\widetilde{\mathrm{grad}}\{\bullet\} \cdot \boldsymbol{m} = \boldsymbol{0}$ and $\widetilde{\mathrm{grad}}\{\bullet\} \cdot \boldsymbol{b} = \boldsymbol{0}$ hold by definition. The curve gradient and curve divergence for tensor valued fields follows from multiplying the tensor valued field $\{\bullet\}$ in Eq. (22) by an arbitrary constant vector.

Remark. Recall the Frénet–Serret formulae for the derivatives of the curve basis vectors

$$\partial_\theta \boldsymbol{t} = \mathsf{c}\,\boldsymbol{m} \quad \text{and} \quad \partial_\theta \boldsymbol{m} = -\mathsf{c}\,\boldsymbol{t} + \mathsf{t}\,\boldsymbol{b} \quad \text{and} \quad \partial_\theta \boldsymbol{b} = -\mathsf{t}\,\boldsymbol{m}. \tag{23}$$

Here c and t denote the scalar valued curvature and torsion of the curve.

Example. Based on the Frénet–Serret formula in Eq. (23.1), the curve divergence of the curve unit or rather projection tensor $\widetilde{\boldsymbol{i}}$ renders

$$\widetilde{\operatorname{div}}\,\widetilde{\boldsymbol{i}} = \mathsf{c}\,\boldsymbol{m}. \tag{24}$$

Likewise, with Eq. (23) the curvature tensors $\boldsymbol{c}_\parallel$, $\boldsymbol{c}_\perp$ and the scalar valued curvature c of the curve $\mathscr{C}$ are defined as the curve gradient of the curve tangent $\boldsymbol{t}$ and the negative curve gradient and curve divergence of the curve normal $\boldsymbol{m}$, respectively,

$$\boldsymbol{c}_\parallel := \widetilde{\operatorname{grad}}\boldsymbol{t} = \partial_\theta \boldsymbol{t} \otimes \boldsymbol{t} \quad \text{and} \quad \boldsymbol{c}_\perp := -\,\widetilde{\operatorname{grad}}\boldsymbol{m} = -\partial_\theta \boldsymbol{m} \otimes \boldsymbol{t}, \tag{25}$$

$$\mathsf{c} := -\,\widetilde{\operatorname{div}}\boldsymbol{m} = -\partial_\theta \boldsymbol{m} \cdot \boldsymbol{t}.$$

The curvature tensors are computed as $\boldsymbol{c}_\parallel = \mathsf{c}\,\boldsymbol{m} \otimes \boldsymbol{t}$ and $\boldsymbol{c}_\perp = \mathsf{c}\,\boldsymbol{t} \otimes \boldsymbol{t} - \mathsf{t}\,\boldsymbol{b} \otimes \boldsymbol{t}$ and live in the planes perpendicular to the binormal $\boldsymbol{b}$ and the (principal) normal $\boldsymbol{m}$, respectively.

With the above terminology and notation we finally recall the:

Curve Divergence Theorem. *Let $\mathscr{C}'$ denote a subcurve of $\mathscr{C}$. The outward normal to the boundary (end) points $\mathscr{P}' := \partial\mathscr{C}'$ of the subcurve $\mathscr{C}'$, living in the cotangent space to $\mathscr{C}'$, is denoted by $\widetilde{\boldsymbol{m}}$. Then the curve divergence theorem for vector valued fields $\{\bullet\}$ reads*

$$\int_{\mathscr{C}'} \widetilde{\operatorname{div}}\{\bullet\}\,\mathrm{d}l = \sum_{\mathscr{P}'} \{\bullet\} \cdot \widetilde{\boldsymbol{m}} - \int_{\mathscr{C}'} \mathsf{c}\,\{\bullet\} \cdot \boldsymbol{m}\,\mathrm{d}l. \tag{26}$$

(To verify the curve divergence theorem (26) for tensor valued fields $\{\bullet\}$ multiply the tensor valued field $\{\bullet\}$ in Eq. (26) by an arbitrary constant vector.) The curve divergence theorem is the specialisation of the ordinary Gauss theorem (or rather the fundamental theorem of calculus) to curves. Especially if the vector field is tangent, i.e. $\{\bullet\} \cdot \boldsymbol{m} = 0$, the similarity is obvious.

Moreover, as a corollary we obtain the:

Point Theorem. *Applying the curve divergence theorem to the curve unit tensor $\widetilde{\boldsymbol{i}}$ renders the point theorem*

$$\int_{\mathscr{C}'} \mathsf{c}\,\boldsymbol{m}\,\mathrm{d}l = \sum_{\mathscr{P}'} \widetilde{\boldsymbol{m}}. \tag{27}$$

As an example for $\mathscr{C}'$ consider a half circle with $\mathsf{c} = 1/r$ and axis of symmetry $\boldsymbol{e}$: the curve integral over $\boldsymbol{m}$ then renders $2r\boldsymbol{e}$, whereas the sum over the end points is computed as $2\boldsymbol{e}$. The point theorem is analogous to the well-known area theorem. Especially if $\mathscr{C}'$ is flat, i.e. $\mathsf{c} = 0$ the similarity is obvious.

For fields that are smooth in a three-dimensional neighbourhood $\mathscr{N}$ of the curve, the curve gradient and curve divergence operators are alternatively defined as

$$\widetilde{\operatorname{grad}}\{\bullet\} := \operatorname{grad}\{\bullet\} \cdot \widetilde{\boldsymbol{i}} \quad \text{and} \quad \widetilde{\operatorname{div}}\{\bullet\} := \widetilde{\operatorname{grad}}\{\bullet\} : \widetilde{\boldsymbol{i}}. \tag{28}$$

Remark. In the sequel we shall distinguish between surfaces/curves $\mathscr{S}_0$, $\mathscr{C}_0$ and $\mathscr{S}_t$, $\mathscr{C}_t$ attached to the material and the spatial configuration $\mathscr{B}_0$ and $\mathscr{B}_t$ of a (deformable) continuum body. The above relations are notationally valid in the spatial configuration, for the same expressions in the material configuration, as a rule, all lower case letters are simply substituted by the corresponding upper case letters.

3. Geometry and kinematics of boundaries

Consider a continuum body that takes the material configuration $\mathcal{B}_0$ at time $t = 0$ and the spatial configuration $\mathcal{B}_t$ at time $t > 0$.[2] The material and the spatial configuration are then identified with all the placements (coordinates in the three-dimensional, embedding euclidian space) $\boldsymbol{X}$ and $\boldsymbol{x}$ that are occupied by the continuum body at time $t = 0$ and $t > 0$, respectively. The placements $\boldsymbol{x}$ and $\boldsymbol{X}$ in the spatial and the material configurations are related by invertible (nonlinear) deformation maps

$$\boldsymbol{x} = \boldsymbol{\varphi}(\boldsymbol{X}) \quad \text{and} \quad \boldsymbol{X} = \boldsymbol{\Phi}(\boldsymbol{x}) \tag{29}$$

with $\boldsymbol{\varphi} = \boldsymbol{\Phi}^{-1}$ and $\boldsymbol{\Phi} = \boldsymbol{\varphi}^{-1}$. The associated deformation gradients or rather (invertible) linear tangent maps relate spatial and material line elements $\mathrm{d}\boldsymbol{x} \in T\mathcal{B}_t$ and $\mathrm{d}\boldsymbol{X} \in T\mathcal{B}_0$ and are defined as

$$\boldsymbol{F} := \mathrm{Grad}\boldsymbol{\varphi}(\boldsymbol{X}) \quad \text{and} \quad \boldsymbol{f} := \mathrm{grad}\boldsymbol{\Phi}(\boldsymbol{x}) \tag{30}$$

with $\boldsymbol{F} = \boldsymbol{f}^{-1} \circ \boldsymbol{\varphi}$ and $\boldsymbol{f} = \boldsymbol{F}^{-1} \circ \boldsymbol{\Phi}$. Consequently, the associated (positive) jacobian determinants[3]or rather (invertible) linear volume maps relate spatial and material volume elements $\mathrm{d}v$ and $\mathrm{d}V$ and are defined as

$$J := \det \boldsymbol{F} > 0 \quad \text{and} \quad j := \det \boldsymbol{f} > 0 \tag{31}$$

with $J = j^{-1} \circ \boldsymbol{\varphi}$ and $j = J^{-1} \circ \boldsymbol{\Phi}$. Likewise, the associated cofactors of the deformation gradients or rather the (invertible) linear area maps relate spatial and material area elements $\mathrm{d}\boldsymbol{a} \in T^*\mathcal{B}_t$ and $\mathrm{d}\boldsymbol{A} \in T^*\mathcal{B}_0$ and are defined as

$$\mathrm{cof}\,\boldsymbol{F} := J\boldsymbol{F}^{-\mathrm{t}} \quad \text{and} \quad \mathrm{cof}\,\boldsymbol{f} := j\boldsymbol{f}^{-\mathrm{t}} \tag{32}$$

with $\mathrm{cof}\,\boldsymbol{F} = [\mathrm{cof}\,\boldsymbol{f}]^{-1} \circ \boldsymbol{\varphi}$ and $\mathrm{cof}\,\boldsymbol{f} = [\mathrm{cof}\,\boldsymbol{F}]^{-1} \circ \boldsymbol{\Phi}$.

The boundary of the continuum body (assumed simply connected) is described (covered) by a patchwork of smooth two-dimensional surfaces in the three-dimensional, embedding euclidian space defined by the zero level sets $S^\varsigma(\boldsymbol{X}) = 0$ of the level set functions $S^\varsigma(\boldsymbol{X})$ for the material configuration and the zero level sets $s^\varsigma(\boldsymbol{x}) = 0$ of the level set functions $s^\varsigma(\boldsymbol{x})$ for the spatial configuration ($\varsigma = 1, n_{\mathrm{surf}}$). With these prescriptions at hand, e.g., the material configuration is defined by

$$\mathcal{B}_0 := \{\boldsymbol{X} | \cap S^\varsigma(\boldsymbol{X}) < 0\}. \tag{33}$$

Then the patchwork of boundary surfaces of, e.g., the material configuration is defined by

$$\mathcal{S}_0 = \cup \mathcal{S}_0^\varsigma := \{\ \boldsymbol{X} \ | \ \cup S^\varsigma(\boldsymbol{X}) = 0\ \} = \partial\mathcal{B}_0, \tag{34}$$

Moreover, the n_{curv} intersections of the n_{surf} individual boundary surface patches define a network of boundary curves ($\kappa = 1, n_{\mathrm{curv}}$), e.g., of the material configuration

$$\mathcal{C}_0 = \cup \mathcal{C}_0^\kappa := \{\boldsymbol{X} | \cap S^\varsigma(\boldsymbol{X}) = 0\} = \cap \mathcal{S}_0^\varsigma. \tag{35}$$

Finally, the n_{poin} intersections of the n_{curv} individual boundary curves define a set of boundary points ($\pi = 1, n_{\mathrm{poin}}$), e.g., of the material configuration

$$\mathcal{P}_0 = \cup \mathcal{P}_0^\pi := \cap\, \mathcal{C}_0^\kappa. \tag{36}$$

The patchwork of surfaces $\mathcal{S}_t$, network of curves $\mathcal{C}_t$ and set of points $\mathcal{P}_t$ of the spatial configuration are defined in analogy.

As necessary preliminaries for the following developments, a number of relevant results pertaining exclusively to the kinematics of the boundary surfaces and boundary curves shall be assembled in the sequel.

[2]Here time is merely understood as a history parameter ordering the sequence of external loading, whereby quasi-static loading conditions are assumed for the sake of simplification.

[3]For later comparisons recall the definition of the (bulk) determinant of the (bulk) deformation gradients

$$\det \boldsymbol{F} := \frac{[\boldsymbol{F}\cdot\boldsymbol{G}_1]\cdot[[\boldsymbol{F}\cdot\boldsymbol{G}_2]\times[\boldsymbol{F}\cdot\boldsymbol{G}_3]]}{\boldsymbol{G}_1\cdot[\boldsymbol{G}_2\times\boldsymbol{G}_3]} \quad \text{and} \quad \det \boldsymbol{f} := \frac{[\boldsymbol{f}\cdot\boldsymbol{g}_1]\cdot[[\boldsymbol{f}\cdot\boldsymbol{g}_2]\times[\boldsymbol{f}\cdot\boldsymbol{g}_3]]}{\boldsymbol{g}_1\cdot[\boldsymbol{g}_2\times\boldsymbol{g}_3]}.$$

3.1. Kinematics of boundary surfaces

Convection of Surface Normals. The boundary surface normals to $\mathcal{S}_0$ and $\mathcal{S}_t$ are convected as

$$\boldsymbol{N} = \boldsymbol{n}\cdot\boldsymbol{F}|\boldsymbol{n}\cdot\boldsymbol{F}|^{-1} \quad \text{with } |\boldsymbol{n}\cdot\boldsymbol{F}| = |\mathrm{Grad}\,\mathrm{S}||\mathrm{grad}\,s|^{-1}, \tag{37}$$

$$\boldsymbol{n} = \boldsymbol{N}\cdot\boldsymbol{f}|\boldsymbol{N}\cdot\boldsymbol{f}|^{-1} \quad \text{with } |\boldsymbol{N}\cdot\boldsymbol{f}| = |\mathrm{grad}\,s||\mathrm{Grad}\,\mathrm{S}|^{-1}.$$

These explicit formats will be relevant in the subsequent derivations.

Proof. Due to convection by the deformation, the level set functions $S(\boldsymbol{X})$ and $s(\boldsymbol{x})$ are related by $S(\boldsymbol{X}) = s(\boldsymbol{x})\circ\boldsymbol{\varphi}(\boldsymbol{X})$ and $s(\boldsymbol{x}) = S(\boldsymbol{X})\circ\boldsymbol{\Phi}(\boldsymbol{x})$, respectively. Thus, the result in Eq. (37) follows directly from the chain rule. □

For notational simplicity the explicit indication of the composition $\circ$ with the deformation maps is omitted in the sequel.

Definition. The spatial variation $\mathrm{D}_\delta\{\bullet\}$ is defined as the variation $\partial_\varepsilon\{\bullet\}(\boldsymbol{\varphi}+\varepsilon\delta\boldsymbol{\varphi};\boldsymbol{X})|_{\varepsilon=0}$ at fixed material placement $\boldsymbol{X}$; the material variation $\mathrm{d}_\delta\{\bullet\}$ is defined as the variation $\partial_\varepsilon\{\bullet\}(\boldsymbol{\Phi}+\varepsilon\delta\boldsymbol{\Phi};\boldsymbol{x})|_{\varepsilon=0}$ at fixed spatial placement $\boldsymbol{x}$.

Theorem. *The spatial variation* $\mathrm{D}_\delta\{\bullet\}$ *of the spatial surface normal* $\boldsymbol{n}$ *and the material variation* $\mathrm{d}_\delta\{\bullet\}$ *of the material surface normal* $\boldsymbol{N}$ *follow as*

$$\mathrm{D}_\delta\boldsymbol{n} = -\boldsymbol{n}\cdot\widehat{\mathrm{grad}}(\mathrm{D}_\delta\boldsymbol{\varphi}) \quad \text{and} \quad \mathrm{d}_\delta\boldsymbol{N} = -\boldsymbol{N}\cdot\widehat{\mathrm{Grad}}(\mathrm{d}_\delta\boldsymbol{\Phi}). \tag{38}$$

Later these results will be particularly important when anisotropic surfaces are considered.

Proof. Applying spatial variations to Eq. (37.3) renders with $\mathrm{D}_\delta\boldsymbol{f} = -\boldsymbol{f}\cdot\mathrm{D}_\delta\boldsymbol{F}\cdot\boldsymbol{f}$ after some algebraic manipulations $\mathrm{D}_\delta\boldsymbol{n} = -\boldsymbol{n}\cdot\mathrm{grad}(\mathrm{D}_\delta\boldsymbol{\varphi}) + [\boldsymbol{n}\otimes\boldsymbol{n}]\cdot[\boldsymbol{n}\cdot\mathrm{grad}(\mathrm{D}_\delta\boldsymbol{\varphi})]$ which, simplified into $\mathrm{D}_\delta\boldsymbol{n} = -[\boldsymbol{n}\cdot\mathrm{grad}(\mathrm{D}_\delta\boldsymbol{\varphi})]\cdot\widehat{\boldsymbol{i}} = -\boldsymbol{n}\cdot\mathrm{grad}(\mathrm{D}_\delta\boldsymbol{\varphi})\cdot\widehat{\boldsymbol{i}}$ proves Eq. (38.1).

Accordingly, applying material variations to Eq. (37.1) renders with $\mathrm{d}_\delta\boldsymbol{F} = -\boldsymbol{F}\cdot\mathrm{d}_\delta\boldsymbol{f}\cdot\boldsymbol{F}$ after some algebraic manipulations $\mathrm{d}_\delta\boldsymbol{N} = -\boldsymbol{N}\cdot\mathrm{Grad}(\mathrm{d}_\delta\boldsymbol{\Phi}) + [\boldsymbol{N}\otimes\boldsymbol{N}]\cdot[\boldsymbol{N}\cdot\mathrm{Grad}(\mathrm{d}_\delta\boldsymbol{\Phi})]$ which, simplified into $\mathrm{d}_\delta\boldsymbol{N} = -[\boldsymbol{N}\cdot\mathrm{Grad}(\mathrm{d}_\delta\boldsymbol{\Phi})]\cdot\widehat{\boldsymbol{I}} = -\boldsymbol{N}\cdot\mathrm{Grad}(\mathrm{d}_\delta\boldsymbol{\Phi})\cdot\widehat{\boldsymbol{I}}$ proves Eq. (38.2). □

Definition. Surface deformation gradients or rather (non-invertible) linear surface tangent maps between line elements $\mathrm{d}\boldsymbol{x}\in T\mathcal{S}_t$ and $\mathrm{d}\boldsymbol{X}\in T\mathcal{S}_0$ are defined as

$$\widehat{\boldsymbol{F}} := \widehat{\mathrm{Grad}}\,\boldsymbol{\varphi}(\boldsymbol{X}) = \boldsymbol{a}_\alpha\otimes\boldsymbol{A}^\alpha \quad \text{and} \quad \widehat{\boldsymbol{f}} := \widehat{\mathrm{grad}}\,\boldsymbol{\Phi}(\boldsymbol{x}) = \boldsymbol{A}_\alpha\otimes\boldsymbol{a}^\alpha. \tag{39}$$

The surface deformation gradients $\widehat{\boldsymbol{F}} = \boldsymbol{F}\cdot\widehat{\boldsymbol{I}}$ and $\widehat{\boldsymbol{f}} = \boldsymbol{f}\cdot\widehat{\boldsymbol{i}}$ are rank deficient and are thus not invertible, nevertheless they are inverse to each other in the following generalised sense

$$\widehat{\boldsymbol{F}}\cdot\widehat{\boldsymbol{f}} = [\boldsymbol{a}_\alpha\otimes\boldsymbol{A}^\alpha]\cdot[\boldsymbol{A}_\beta\otimes\boldsymbol{a}^\beta] = \widehat{\boldsymbol{i}} \quad \text{and} \quad \widehat{\boldsymbol{f}}\cdot\widehat{\boldsymbol{F}} = [\boldsymbol{A}_\alpha\otimes\boldsymbol{a}^\alpha]\cdot[\boldsymbol{a}_\beta\otimes\boldsymbol{A}^\beta] = \widehat{\boldsymbol{I}}. \tag{40}$$

Moreover, the following identities hold, highlighting that the surface deformation gradients indeed map between the tangent spaces $T\mathcal{S}_0$ and $T\mathcal{S}_t$

$$\widehat{\boldsymbol{F}}\cdot\widehat{\boldsymbol{I}} \equiv \widehat{\boldsymbol{F}} \quad \text{and} \quad \widehat{\boldsymbol{i}}\cdot\widehat{\boldsymbol{F}} \equiv \widehat{\boldsymbol{F}} \quad \text{and} \quad \widehat{\boldsymbol{f}}\cdot\widehat{\boldsymbol{i}} \equiv \widehat{\boldsymbol{f}} \quad \text{and} \quad \widehat{\boldsymbol{I}}\cdot\widehat{\boldsymbol{f}} \equiv \widehat{\boldsymbol{f}}. \tag{41}$$

The surface deformation gradients are the prime kinematic quantities when it comes to the definition of surface potentials.

Corollary. *The appropriate variations of the surface deformation gradients* $\widehat{\boldsymbol{F}}$ *and* $\widehat{\boldsymbol{f}}$ *are related by*

$$\widehat{\boldsymbol{i}}\cdot\mathrm{d}_\delta\widehat{\boldsymbol{F}}\cdot\widehat{\boldsymbol{I}} = -\widehat{\boldsymbol{F}}\cdot\mathrm{d}_\delta\widehat{\boldsymbol{f}}\cdot\widehat{\boldsymbol{F}} \quad \textit{and} \quad \widehat{\boldsymbol{I}}\cdot\mathrm{D}_\delta\widehat{\boldsymbol{f}}\cdot\widehat{\boldsymbol{i}} = -\widehat{\boldsymbol{f}}\cdot\mathrm{D}_\delta\widehat{\boldsymbol{F}}\cdot\widehat{\boldsymbol{f}} \tag{42}$$

These results correspond to the relations $\mathrm{d}_\delta\boldsymbol{A}^\alpha\cdot\boldsymbol{A}_\beta = -\boldsymbol{A}^\alpha\cdot\mathrm{d}_\delta\boldsymbol{A}_\beta$ *and* $\mathrm{D}_\delta\boldsymbol{a}^\alpha\cdot\boldsymbol{a}_\beta = -\boldsymbol{a}^\alpha\cdot\mathrm{D}_\delta\boldsymbol{a}_\beta$.

Proof. Taking the material variation $\mathrm{d}_\delta\{\bullet\}$ of Eq. (40.1) and the spatial variation $\mathrm{D}_\delta\{\bullet\}$ of Eq. (40.2) and multiplying the result from the right by $\widehat{\boldsymbol{F}}$ and $\widehat{\boldsymbol{f}}$, repectively, renders together with Eqs. (40), (41) immediately the above result.

Alternatively, applying the appropriate variations to the surface deformation gradients expressed by the surface basis vectors as in Eq. (39) proves again the result in Eq. (42). □

Surface Area Maps. Surface area elements $\mathrm{d}A$ and $\mathrm{d}a$ of $\mathscr{S}_0$ and $\mathscr{S}_t$ are mapped into each other by the surface Jacobians $\widehat{J}$ and $\widehat{j}$ as

$$\mathrm{d}a = \widehat{J}\,\mathrm{d}A \quad \text{and} \quad \mathrm{d}A = \widehat{j}\,\mathrm{d}a \tag{43}$$

with

$$\widehat{J} = \widehat{\det}\,\widehat{\boldsymbol{F}} := |\mathrm{cof}\,\boldsymbol{F}\cdot\boldsymbol{N}| \quad \text{and} \quad \widehat{j} = \widehat{\det}\widehat{\boldsymbol{f}} := |\mathrm{cof}\,\boldsymbol{f}\cdot\boldsymbol{n}|. \tag{44}$$

Clearly, due to Eqs. (32), (37) the surface Jacobians $\widehat{J}$ and $\widehat{j}$ are inverse to each other.

Proof. The Nanson formula relates oriented surface area elements $\mathrm{d}\boldsymbol{A}$ and $\mathrm{d}\boldsymbol{a}$ in $T^*\mathscr{B}_0$ and $T^*\mathscr{B}_t$

$$\boldsymbol{n}\,\mathrm{d}a = \mathrm{cof}\,\boldsymbol{F}\cdot\boldsymbol{N}\,\mathrm{d}A \quad \text{and} \quad \boldsymbol{N}\,\mathrm{d}A = \mathrm{cof}\,\boldsymbol{f}\cdot\boldsymbol{n}\,\mathrm{d}a. \tag{45}$$

Thus the relation between the surface area elements in Eq. (43) is the scalar version of Eq. (45).

Alternatively, simply take the ratio of surface area elements $\mathrm{d}a$ and $\mathrm{d}A$ as expressed in Eq. (6). Thus, based on the surface metric coefficients as in (3), (5), (6), we express the surface Jacobians as $\widehat{J} = [\det[a_{\alpha\beta}]/\det[A_{\alpha\beta}]]^{1/2} = [a^{33}/A^{33}]^{1/2} = \widehat{j}^{-1}$. This renders eventually the definition of the surface determinant of the surface deformation gradients, see also Gurtin and Struthers (1990), as

$$\widehat{\det}\,\widehat{\boldsymbol{F}} := \frac{|[\widehat{\boldsymbol{F}}\cdot\boldsymbol{A}_1]\times[\widehat{\boldsymbol{F}}\cdot\boldsymbol{A}_2]|}{|\boldsymbol{A}_1\times\boldsymbol{A}_2|} \quad \textit{and} \quad \widehat{\det}\widehat{\boldsymbol{f}} := \frac{|[\widehat{\boldsymbol{f}}\cdot\boldsymbol{a}_1]\times[\widehat{\boldsymbol{f}}\cdot\boldsymbol{a}_2]|}{|\boldsymbol{a}_1\times\boldsymbol{a}_2|}. \tag{46}$$

Observe the relation to the (bulk) determinant of the (bulk) deformation gradients in Footnote 3. Note further $\widehat{\boldsymbol{F}}\cdot\boldsymbol{A}_\alpha = \boldsymbol{F}\cdot\boldsymbol{A}_\alpha$ and $\widehat{\boldsymbol{f}}\cdot\boldsymbol{a}_\alpha = \boldsymbol{f}\cdot\boldsymbol{a}_\alpha$ so that $[\widehat{\boldsymbol{F}}\cdot\boldsymbol{A}_1]\times[\widehat{\boldsymbol{F}}\cdot\boldsymbol{A}_2] = \mathrm{cof}\,\boldsymbol{F}\cdot[\boldsymbol{A}_1\times\boldsymbol{A}_2] = \mathrm{cof}\,\boldsymbol{F}\cdot\boldsymbol{N}\,|\boldsymbol{A}_1\times\boldsymbol{A}_2|$ and $[\widehat{\boldsymbol{f}}\cdot\boldsymbol{a}_1]\times[\widehat{\boldsymbol{f}}\cdot\boldsymbol{a}_2] = \mathrm{cof}\,\boldsymbol{f}\cdot[\boldsymbol{a}_1\times\boldsymbol{a}_2] = \mathrm{cof}\,\boldsymbol{f}\cdot\boldsymbol{n}\,|\boldsymbol{a}_1\times\boldsymbol{a}_2|$. □

Corollary. *The spatial variation* $\mathrm{D}_\delta\{\bullet\}$ *of the surface Jacobian* $\widehat{J}$ *and the material variation* $\mathrm{d}_\delta\{\bullet\}$ *of the surface Jacobian* $\widehat{j}$ *follow as*

$$\mathrm{D}_\delta\widehat{J} = \widehat{J}\,\widehat{\mathrm{div}}(\mathrm{D}_\delta\boldsymbol{\varphi}) \quad \textit{and} \quad \mathrm{d}_\delta\widehat{j} = \widehat{j}\,\widehat{\mathrm{Div}}(\mathrm{d}_\delta\boldsymbol{\Phi}). \tag{47}$$

Observe the intriguing formal similarity to the appropriate variations of the bulk Jacobians.

Proof. The surface Jacobian $\widehat{J}$ is expressed as $\widehat{J} = J\,N$ with $N := |\boldsymbol{N}\cdot\boldsymbol{f}|$. The spatial variation of the bulk Jacobian J is given by $\mathrm{D}_\delta J = J\boldsymbol{i} : \mathrm{grad}(\mathrm{D}_\delta\boldsymbol{\varphi})$. The spatial variation of N follows with the chain rule and Eq. (37.3) as $\mathrm{D}_\delta N = \boldsymbol{n}\cdot\,\mathrm{D}_\delta[\boldsymbol{N}\cdot\boldsymbol{f}] = -N\,[\boldsymbol{n}\otimes\boldsymbol{n}] : \mathrm{grad}(\mathrm{D}_\delta\boldsymbol{\varphi})$. Combining the previous results renders Eq. (47.1) in the format $\mathrm{D}_\delta\widehat{J} = \widehat{J}\,\widehat{\boldsymbol{i}} : \widehat{\mathrm{grad}}(\mathrm{D}_\delta\boldsymbol{\varphi})$.

Accordingly, the surface Jacobian $\widehat{j}$ is expressed as $\widehat{j} = j\,n$ with $n := |\boldsymbol{n}\cdot\boldsymbol{F}|$. The material variation of the bulk Jacobian j is given by $\mathrm{d}_\delta j = j\boldsymbol{I} : \mathrm{Grad}(\mathrm{d}_\delta\boldsymbol{\Phi})$. The material variation of n follows with the chain rule and Eq. (37.1) as $\mathrm{d}_\delta n = \boldsymbol{N}\cdot\,\mathrm{d}_\delta[\boldsymbol{n}\cdot\boldsymbol{F}] = -n\,[\boldsymbol{N}\otimes\boldsymbol{N}] : \mathrm{Grad}(\mathrm{d}_\delta\boldsymbol{\Phi})$. Combining the previous results renders Eq. (47.2) in the format $\mathrm{d}_\delta\widehat{j} = \widehat{j}\,\widehat{\boldsymbol{I}} : \widehat{\mathrm{Grad}}(\mathrm{d}_\delta\boldsymbol{\Phi})$. □

Corollary. *The derivatives of the surface Jacobians* $\widehat{J} = \widehat{J}(\boldsymbol{F},\boldsymbol{N})$ *and* $\widehat{j} = \widehat{j}(\boldsymbol{f},\boldsymbol{n})$ *with respect to the surface deformation gradients* $\widehat{\boldsymbol{F}}$ *and* $\widehat{\boldsymbol{f}}$ *are given by*

$$\partial_{\widehat{\boldsymbol{F}}}\widehat{J} = \widehat{J}\,\widehat{\boldsymbol{f}}^{\mathrm{t}} \quad \textit{and} \quad \partial_{\widehat{\boldsymbol{f}}}\widehat{j} = \widehat{j}\,\widehat{\boldsymbol{F}}^{\mathrm{t}}. \tag{48}$$

Observe the formal similarity to the derivatives of the bulk Jacobians with respect to the bulk deformation gradients.

Proof. With $\mathrm{D}_\delta \widehat{J} = \widehat{J}\widehat{\boldsymbol{i}} : \widehat{\mathrm{grad}}(\mathrm{D}_\delta \boldsymbol{\varphi}) = \widehat{J}\widehat{\boldsymbol{f}}^{\mathrm{t}} : \mathrm{D}_\delta \widehat{\boldsymbol{F}}$ and $\mathrm{d}_\delta \widehat{j} = \widehat{j}\widehat{\boldsymbol{I}} : \widehat{\mathrm{Grad}}(\mathrm{d}_\delta \boldsymbol{\Phi}) = \widehat{j}\widehat{\boldsymbol{F}}^{\mathrm{t}} : \mathrm{d}_\delta \widehat{\boldsymbol{f}}$ the result in Eq. (48) follows immediately. □

Surface Nanson Formula. The oriented line elements $\mathrm{d}\widehat{\boldsymbol{L}} = \widehat{\boldsymbol{N}}\,\mathrm{d}L$ and $\mathrm{d}\widehat{\boldsymbol{l}} = \widehat{\boldsymbol{n}}\,\mathrm{d}l$ in $T^*\mathscr{S}_0$ and $T^*\mathscr{S}_t$ are related by a surface version of the Nanson formula

$$\widehat{\boldsymbol{n}}\,\mathrm{d}l = \widehat{\mathrm{cof}}\,\widehat{\boldsymbol{F}} \cdot \widehat{\boldsymbol{N}}\,\mathrm{d}L \quad \text{and} \quad \widehat{\boldsymbol{N}}\,\mathrm{d}L = \widehat{\mathrm{cof}}\,\widehat{\boldsymbol{f}} \cdot \widehat{\boldsymbol{n}}\,\mathrm{d}l \tag{49}$$

with

$$\widehat{\mathrm{cof}}\,\widehat{\boldsymbol{F}} := \widehat{J}\widehat{\boldsymbol{f}}^{\mathrm{t}} \quad \text{and} \quad \widehat{\mathrm{cof}}\,\widehat{\boldsymbol{f}} := \widehat{j}\widehat{\boldsymbol{F}}^{\mathrm{t}}. \tag{50}$$

Here the definition of the surface cofactor $\widehat{\mathrm{cof}}\{\bullet\}$ of the surface deformation gradient should not be confused with the cofactor of a rank deficient tensor as given in Proposition 1.1.5 of Šilhavý (1997).

Proof. The area element $\mathrm{d}A$ of $\mathscr{S}'_0$ (considered as parallelogram) touching the boundary curve $\mathscr{C}'_0$ is spanned by the length of the line element $\mathrm{d}L$ tangent to $\mathscr{C}'_0$ and the height $\mathrm{d}H$ of the area element parallelogram perpendicular to $\mathscr{C}'_0$ as $\mathrm{d}A = \mathrm{d}H\,\mathrm{d}L$. The ratio of the area elements $\mathrm{d}A$ and $\mathrm{d}a$ is given by Eq. (43) in terms of the surface Jacobian as $\mathrm{d}a = \widehat{J}\,\mathrm{d}A$. The line element $\widehat{\boldsymbol{T}}$ in $T\mathscr{S}'_0$ with $|\widehat{\boldsymbol{T}}| = \mathrm{d}H$, initially perpendicular to $\mathscr{C}'_0$, is convected by the deformation as $\widehat{\boldsymbol{T}} \mapsto \widehat{\boldsymbol{F}} \cdot \widehat{\boldsymbol{T}}$. The convected line element is in general not perpendicular to $\mathscr{C}'_t$ anymore. Thus the height $\mathrm{d}h$ of the convected area element is computed as $\mathrm{d}h = \widehat{\boldsymbol{n}} \cdot \widehat{\boldsymbol{F}} \cdot \widehat{\boldsymbol{T}}$. The normal $\widehat{\boldsymbol{n}}$ to $\mathscr{C}'_t$ and tangent to $\mathscr{S}'_t$ is given by $\widehat{\boldsymbol{n}} = \widehat{\boldsymbol{N}} \cdot \widehat{\boldsymbol{f}}\,|\widehat{\boldsymbol{N}} \cdot \widehat{\boldsymbol{f}}|^{-1}$. Thus the height $\mathrm{d}h$ follows as $\mathrm{d}h = |\widehat{\boldsymbol{N}} \cdot \widehat{\boldsymbol{f}}|^{-1}\,\mathrm{d}H$.

Likewise, the area element $\mathrm{d}a$ of $\mathscr{S}'_t$ (considered as parallelograms) touching the boundary curve $\mathscr{C}'_t$ is spanned by the length of the line element $\mathrm{d}l$ tangent to $\mathscr{C}'_t$ and the height $\mathrm{d}h$ of the area element parallelogram perpendicular to $\mathscr{C}'_t$ as $\mathrm{d}a = \mathrm{d}h\,\mathrm{d}l$. The ratio of the area elements $\mathrm{d}a$ and $\mathrm{d}A$ is given by Eq. (43) in terms of the surface Jacobian as $\mathrm{d}A = \widehat{j}\,\mathrm{d}a$. The line element $\widehat{\boldsymbol{t}}$ in $T\mathscr{S}'_t$ with $|\widehat{\boldsymbol{t}}| = \mathrm{d}h$, initially perpendicular to $\mathscr{C}'_t$, is convected by the deformation as $\widehat{\boldsymbol{t}} \mapsto \widehat{\boldsymbol{f}} \cdot \widehat{\boldsymbol{t}}$. The convected line element is in general not perpendicular to $\mathscr{C}'_0$ anymore. Thus the height $\mathrm{d}H$ of the convected area element is computed as $\mathrm{d}H = \widehat{\boldsymbol{N}} \cdot \widehat{\boldsymbol{f}} \cdot \widehat{\boldsymbol{t}}$.The normal $\widehat{\boldsymbol{N}}$ to $\mathscr{C}'_0$ and tangent to $\mathscr{S}'_0$ is given by $\widehat{\boldsymbol{N}} = \widehat{\boldsymbol{n}} \cdot \widehat{\boldsymbol{F}}\,|\widehat{\boldsymbol{n}} \cdot \widehat{\boldsymbol{F}}|^{-1}$. Thus the height $\mathrm{d}H$ follows as $\mathrm{d}H = |\widehat{\boldsymbol{n}} \cdot \widehat{\boldsymbol{F}}|^{-1}\,\mathrm{d}h$.

Finally the ratio of line elements $\mathrm{d}L$ and $\mathrm{d}l$ is computed as

$$\frac{\mathrm{d}l}{\mathrm{d}L} = \frac{\mathrm{d}a}{\mathrm{d}A}\frac{\mathrm{d}H}{\mathrm{d}h} = |\widehat{\mathrm{cof}}\,\widehat{\boldsymbol{F}} \cdot \widehat{\boldsymbol{N}}| \quad \text{and} \quad \frac{\mathrm{d}L}{\mathrm{d}l} = \frac{\mathrm{d}A}{\mathrm{d}a}\frac{\mathrm{d}h}{\mathrm{d}H} = |\widehat{\mathrm{cof}}\,\widehat{\boldsymbol{f}} \cdot \widehat{\boldsymbol{n}}|. \tag{51}$$

Clearly this is the scalar version of Eq. (49) in the sense of absolute values. □

Surface Piola Identity. The surface Piola identity gives an expression for the surface divergence of the surface cofactor of the surface deformation gradient

$$\widehat{\mathrm{Div}}(\widehat{\mathrm{cof}}\,\widehat{\boldsymbol{F}}) = \widehat{J}k\boldsymbol{n} \quad \text{and} \quad \widehat{\mathrm{div}}(\widehat{\mathrm{cof}}\,\widehat{\boldsymbol{f}}) = \widehat{j}K\boldsymbol{N}. \tag{52}$$

The surface Piola identity is the specialisation of the ordinary Piola identity to surfaces. Especially if the surface is flat in both configurations, i.e. $k = 0$ and $K = 0$, the similarity is obvious.

Proof. Since $\widehat{\mathrm{cof}}\,\widehat{\boldsymbol{F}} \cdot \boldsymbol{N} = \boldsymbol{0}$ and $\widehat{\mathrm{cof}}\,\widehat{\boldsymbol{f}} \cdot \boldsymbol{n} = \boldsymbol{0}$ the surface divergence theorem in Eq. (12) renders

$$\int_{\mathscr{S}'_0} \widehat{\mathrm{Div}}(\widehat{\mathrm{cof}}\,\widehat{\boldsymbol{F}})\,\mathrm{d}A = \int_{\mathscr{C}'_0} \widehat{\mathrm{cof}}\,\widehat{\boldsymbol{F}} \cdot \widehat{\boldsymbol{N}}\,\mathrm{d}L, \quad \int_{\mathscr{S}'_t} \widehat{\mathrm{div}}(\widehat{\mathrm{cof}}\,\widehat{\boldsymbol{f}})\,\mathrm{d}a = \int_{\mathscr{C}'_t} \widehat{\mathrm{cof}}\,\widehat{\boldsymbol{f}} \cdot \widehat{\boldsymbol{n}}\,\mathrm{d}l. \tag{53}$$

With the surface Nanson formula in Eq. (49) and the line theorem in Eq. (13) the surface Piola identity is finally obtained from Eq. (53). □

Surface Piola Transforms. For surface quantities $\{\bullet\}$ related by surface Piola transforms $\{\bullet\} \mapsto \{\bullet\} \cdot \widehat{\mathrm{cof}}\,\widehat{\boldsymbol{F}}$ and $\{\bullet\} \mapsto \{\bullet\} \cdot \widehat{\mathrm{cof}}\,\widehat{\boldsymbol{f}}$ the surface Piola identity renders

$$\widehat{\mathrm{Div}}(\{\bullet\} \cdot \widehat{\mathrm{cof}}\,\widehat{\boldsymbol{F}}) = \widehat{J}[\widehat{\mathrm{div}}(\{\bullet\}) + k\{\bullet\} \cdot \boldsymbol{n}] \tag{54}$$

and

$$\widehat{\operatorname{div}}(\{\bullet\}\cdot\widehat{\operatorname{cof}}\widehat{\boldsymbol{f}}) = \widehat{j}[\widehat{\operatorname{Div}}(\{\bullet\}) + K\{\bullet\}\cdot\boldsymbol{N}].$$

Surface Piola transforms are the specialisation of the ordinary Piola transforms to surfaces. Especially if the surface is flat in both configurations, i.e. $k = 0$ and $K = 0$, or the $\{\bullet\}$ are tangent, i.e. $\{\bullet\}\cdot\boldsymbol{n} = 0$ or $\{\bullet\}\cdot\boldsymbol{N} = 0$, respectively, the similarity is obvious.

3.2. Kinematics of boundary curves

Convection of Curve Tangent. The boundary curve tangents to $\mathscr{C}_0$ and $\mathscr{C}_t$ are convected as

$$\boldsymbol{T} = \frac{\boldsymbol{f}\cdot\boldsymbol{t}}{|\boldsymbol{f}\cdot\boldsymbol{t}|} \quad \text{and} \quad \boldsymbol{t} = \frac{\boldsymbol{F}\cdot\boldsymbol{T}}{|\boldsymbol{F}\cdot\boldsymbol{T}|}. \tag{55}$$

These explicit formats will be relevant in the subsequent derivations.

Theorem. *The spatial variation* $\mathrm{D}_\delta\{\bullet\}$ *of the spatial curve tangent* $\boldsymbol{t}$ *and the material variation* $\mathrm{d}_\delta\{\bullet\}$ *of the material curve tangent* $\boldsymbol{T}$ *follow as*

$$\mathrm{D}_\delta\boldsymbol{t} = [\widetilde{\boldsymbol{i}}^{\perp}\otimes\boldsymbol{t}] : \widetilde{\operatorname{grad}}(\mathrm{D}_\delta\boldsymbol{\varphi}) \quad \textit{and} \quad \mathrm{d}_\delta\boldsymbol{T} = [\widetilde{\boldsymbol{I}}^{\perp}\otimes\boldsymbol{T}] : \widetilde{\operatorname{Grad}}(\mathrm{d}_\delta\boldsymbol{\Phi}). \tag{56}$$

Here $\widetilde{\boldsymbol{i}}^{\perp} := \boldsymbol{i} - \widetilde{\boldsymbol{i}}$ *and* $\widetilde{\boldsymbol{I}}^{\perp} := \boldsymbol{I} - \widetilde{\boldsymbol{I}}$ *are projections to the plane perpendicular to* $\boldsymbol{t}$ *and* $\boldsymbol{T}$, *respectively. Later these results will be particularly important when anisotropic curves are considered.*

Proof. Applying spatial variations to Eq. (55.2) renders after some algebraic manipulations $\mathrm{D}_\delta\boldsymbol{t} = \operatorname{grad}(\mathrm{D}_\delta\boldsymbol{\varphi})\cdot\boldsymbol{t} - [\boldsymbol{t}\otimes\boldsymbol{t}]\cdot\operatorname{grad}(\mathrm{D}_\delta\boldsymbol{\varphi})\cdot\boldsymbol{t}$ which, modified into $\mathrm{D}_\delta\boldsymbol{t} = [[\boldsymbol{i} - \boldsymbol{t}\otimes\boldsymbol{t}]\otimes\boldsymbol{t}] : [\operatorname{grad}(\mathrm{D}_\delta\boldsymbol{\varphi})\cdot[\boldsymbol{t}\otimes\boldsymbol{t}]]$ proves Eq. (56.1).

Accordingly, applying material variations to Eq. (55.1) renders after some algebraic manipulations $\mathrm{d}_\delta\boldsymbol{T} = \operatorname{Grad}(\mathrm{d}_\delta\boldsymbol{\Phi})\cdot\boldsymbol{T} - [\boldsymbol{T}\otimes\boldsymbol{T}]\cdot\operatorname{Grad}(\mathrm{d}_\delta\boldsymbol{\Phi})\cdot\boldsymbol{T}$ which, modified into $\mathrm{d}_\delta\boldsymbol{T} = [[\boldsymbol{I} - \boldsymbol{T}\otimes\boldsymbol{T}]\otimes\boldsymbol{T}] : [\operatorname{Grad}(\mathrm{d}_\delta\boldsymbol{\Phi})\cdot[\boldsymbol{T}\otimes\boldsymbol{T}]]$ proves Eq. (56.2). □

Definition. Curve deformation gradients or rather (non-invertible) linear curve tangent maps between line elements $\mathrm{d}\boldsymbol{x}\in T\mathscr{C}_t$ and $\mathrm{d}\boldsymbol{X}\in T\mathscr{C}_0$ are defined as

$$\widetilde{\boldsymbol{F}} := \widetilde{\operatorname{Grad}}\,\boldsymbol{\varphi}(\boldsymbol{X}) = \lambda\,\boldsymbol{t}\otimes\boldsymbol{T} \quad \text{and} \quad \widetilde{\boldsymbol{f}} := \widetilde{\operatorname{grad}}\boldsymbol{\Phi}(\boldsymbol{x}) = \Lambda\,\boldsymbol{T}\otimes\boldsymbol{t}. \tag{57}$$

Here $\lambda = \mathrm{d}l/\mathrm{d}L = \Lambda^{-1}$ denotes the curve stretch. The curve deformation gradients $\widetilde{\boldsymbol{F}} = \boldsymbol{F}\cdot\widetilde{\boldsymbol{I}}$ and $\widetilde{\boldsymbol{f}} = \boldsymbol{f}\cdot\widetilde{\boldsymbol{i}}$ are rank deficient and are thus not invertible, nevertheless they are inverse to each other in the following generalised sense

$$\widetilde{\boldsymbol{F}}\cdot\widetilde{\boldsymbol{f}} = \lambda\Lambda[\boldsymbol{t}\otimes\boldsymbol{T}]\cdot[\boldsymbol{T}\otimes\boldsymbol{t}] = \widetilde{\boldsymbol{i}} \quad \text{and} \quad \widetilde{\boldsymbol{f}}\cdot\widetilde{\boldsymbol{F}} = \Lambda\lambda[\boldsymbol{T}\otimes\boldsymbol{t}]\cdot[\boldsymbol{t}\otimes\boldsymbol{T}] = \widetilde{\boldsymbol{I}}. \tag{58}$$

Moreover, the following identities hold, highlighting that the curve deformation gradients indeed map between the tangent spaces $T\mathscr{C}_0$ and $T\mathscr{C}_t$

$$\widetilde{\boldsymbol{F}}\cdot\widetilde{\boldsymbol{I}} \equiv \widetilde{\boldsymbol{F}} \quad \text{and} \quad \widetilde{\boldsymbol{i}}\cdot\widetilde{\boldsymbol{F}} \equiv \widetilde{\boldsymbol{F}} \quad \text{and} \quad \widetilde{\boldsymbol{f}}\cdot\widetilde{\boldsymbol{i}} \equiv \widetilde{\boldsymbol{f}} \quad \text{and} \quad \widetilde{\boldsymbol{I}}\cdot\widetilde{\boldsymbol{f}} \equiv \widetilde{\boldsymbol{f}}. \tag{59}$$

The curve deformation gradients are the prime kinematic quantities when it comes to the definition of curve potentials.

Corollary. *The appropriate variations of the curve deformation gradients* $\widetilde{\boldsymbol{F}}$ *and* $\widetilde{\boldsymbol{f}}$ *are related by*

$$\widetilde{\boldsymbol{i}}\cdot\mathrm{d}_\delta\widetilde{\boldsymbol{F}}\cdot\widetilde{\boldsymbol{I}} = -\widetilde{\boldsymbol{F}}\cdot\mathrm{d}_\delta\widetilde{\boldsymbol{f}}\cdot\widetilde{\boldsymbol{F}} \quad \textit{and} \quad \widetilde{\boldsymbol{I}}\cdot\mathrm{D}_\delta\widetilde{\boldsymbol{f}}\cdot\widetilde{\boldsymbol{i}} = -\widetilde{\boldsymbol{f}}\cdot\mathrm{D}_\delta\widetilde{\boldsymbol{F}}\cdot\widetilde{\boldsymbol{f}}. \tag{60}$$

These results correspond to the relations $\mathrm{d}_\delta\lambda = -\lambda^2\,\mathrm{d}_\delta\Lambda$ *and* $\mathrm{D}_\delta\Lambda = -\Lambda^2\,\mathrm{D}_\delta\lambda$.

Proof. Taking the material variation $\mathrm{d}_\delta\{\bullet\}$ of Eq. (58.1) and the spatial variation $\mathrm{D}_\delta\{\bullet\}$ of Eq. (58.2) and multiplying the result from the right by $\widetilde{\boldsymbol{F}}$ and $\widetilde{\boldsymbol{f}}$, respectively, renders together with Eqs. (58), (59) immediately the above result. □

Curve Line Maps. Curve line elements $\mathrm{d}L$ and $\mathrm{d}l$ of $\mathscr{C}_0$ and $\mathscr{C}_t$ are obviously mapped into each other by the curve Jacobians $\widetilde{J}$ and $\widetilde{j}$ as

$$\mathrm{d}l = \widetilde{J}\,\mathrm{d}L \quad \text{and} \quad \mathrm{d}L = \widetilde{j}\,\mathrm{d}l, \tag{61}$$

with

$$\widetilde{J} = \widetilde{\det}\,\widetilde{\boldsymbol{F}} := |\boldsymbol{F}\cdot\boldsymbol{T}| \quad \text{and} \quad \widetilde{j} = \widetilde{\det}\,\widetilde{\boldsymbol{f}} := |\boldsymbol{f}\cdot\boldsymbol{t}|. \tag{62}$$

Here, with $\boldsymbol{F}\cdot\boldsymbol{T} = \widetilde{\boldsymbol{F}}\cdot\boldsymbol{T}$ and $\boldsymbol{f}\cdot\boldsymbol{t} = \widetilde{\boldsymbol{f}}\cdot\boldsymbol{t}$ the curve determinant of the curve deformation gradients is defined as

$$\widetilde{\det}\,\widetilde{\boldsymbol{F}} := \frac{|\widetilde{\boldsymbol{F}}\cdot\boldsymbol{T}|}{|\boldsymbol{T}|} \quad \text{and} \quad \widetilde{\det}\,\widetilde{\boldsymbol{f}} := \frac{|\widetilde{\boldsymbol{f}}\cdot\boldsymbol{t}|}{|\boldsymbol{t}|}. \tag{63}$$

For a comparison recall the relation to the (bulk) determinant of the (bulk) deformation gradient in Footnote 3 or the corresponding formulation for surface quantities in Eq. (46). Observe that the curve Jacobians $\widetilde{J}$ and $\widetilde{j}$ are inverse to each other.

Corollary. *The spatial variation* $\mathrm{D}_\delta\{\bullet\}$ *of the curve Jacobian* $\widetilde{J}$ *and the material variation* $\mathrm{d}_\delta\{\bullet\}$ *of the curve Jacobian* $\widetilde{j}$ *follow as*

$$\mathrm{D}_\delta\widetilde{J} = \widetilde{J}\,\widetilde{\mathrm{div}}(\mathrm{D}_\delta\boldsymbol{\varphi}) \quad \textit{and} \quad \mathrm{d}_\delta\widetilde{j} = \widetilde{j}\,\widetilde{\mathrm{Div}}(\mathrm{d}_\delta\boldsymbol{\Phi}). \tag{64}$$

Observe the intriguing formal similarity to the appropriate variations of the bulk and surface Jacobians.

Proof. The curve Jacobian $\widetilde{J}$ is expressed as $\widetilde{J} = |\widetilde{\boldsymbol{F}}\cdot\boldsymbol{T}|$. The spatial variation of $\widetilde{J}$ follows as $\mathrm{D}_\delta\widetilde{J} = \boldsymbol{t}\cdot \mathrm{D}_\delta\widetilde{\boldsymbol{F}}\cdot\boldsymbol{T}$ which renders Eq. (64.1) in the format $\mathrm{D}_\delta\widetilde{J} = [\boldsymbol{t}\otimes\boldsymbol{t}] : [\widetilde{\mathrm{Grad}}(\mathrm{D}_\delta\boldsymbol{\varphi})\cdot[\boldsymbol{T}\otimes\boldsymbol{t}]]$.

Accordingly, the curve Jacobian $\widetilde{j}$ is expressed as $\widetilde{j} = |\widetilde{\boldsymbol{f}}\cdot\boldsymbol{t}|$. The material variation of $\widetilde{j}$ follows as $\mathrm{d}_\delta\widetilde{j} = \boldsymbol{T}\cdot\mathrm{d}_\delta\widetilde{\boldsymbol{f}}\cdot\boldsymbol{t}$ which renders Eq. (64.2) in the format $\mathrm{d}_\delta\widetilde{j} = [\boldsymbol{T}\otimes\boldsymbol{T}] : [\widetilde{\mathrm{grad}}(\mathrm{d}_\delta\boldsymbol{\Phi})\cdot[\boldsymbol{t}\otimes\boldsymbol{T}]]$. □

Corollary. *The derivatives of the curve Jacobians* $\widetilde{J} = \widetilde{J}(\boldsymbol{F},\boldsymbol{T})$ *and* $\widetilde{j} = \widetilde{j}(\boldsymbol{f},\boldsymbol{t})$ *with respect to the curve deformation gradients* $\widetilde{\boldsymbol{F}}$ *and* $\widetilde{\boldsymbol{f}}$ *are given by*

$$\partial_{\widetilde{\boldsymbol{F}}}\widetilde{J} = \widetilde{J}\widetilde{\boldsymbol{f}}^{\mathrm{t}} \quad \textit{and} \quad \partial_{\widetilde{\boldsymbol{f}}}\widetilde{j} = \widetilde{j}\widetilde{\boldsymbol{F}}^{\mathrm{t}}. \tag{65}$$

Observe the formal similarity to the derivatives of the bulk Jacobians with respect to the bulk deformation gradients.

Proof. With $\mathrm{D}_\delta\widetilde{J} = \widetilde{J}\widetilde{\boldsymbol{i}} : \widetilde{\mathrm{grad}}(\mathrm{D}_\delta\boldsymbol{\varphi}) = \widetilde{J}\widetilde{\boldsymbol{f}}^{\mathrm{t}} : \mathrm{D}_\delta\widetilde{\boldsymbol{F}}$ and $\mathrm{d}_\delta\widetilde{j} = \widetilde{j}\widetilde{\boldsymbol{I}} : \widetilde{\mathrm{Grad}}(\mathrm{d}_\delta\boldsymbol{\Phi}) = \widetilde{j}\widetilde{\boldsymbol{F}}^{\mathrm{t}} : \mathrm{d}_\delta\widetilde{\boldsymbol{f}}$ the result in Eq. (65) follows immediately. □

Curve Nanson Formula. The oriented point elements $\widetilde{\boldsymbol{M}}$ and $\widetilde{\boldsymbol{m}}$ in $T^*\mathscr{C}_0$ and $T^*\mathscr{C}_t$ are related by a curve version of the Nanson formula

$$\widetilde{\boldsymbol{m}} = \widetilde{\mathrm{cof}}\,\widetilde{\boldsymbol{F}}\cdot\widetilde{\boldsymbol{M}} \quad \text{and} \quad \widetilde{\boldsymbol{M}} = \widetilde{\mathrm{cof}}\,\widetilde{\boldsymbol{f}}\cdot\widetilde{\boldsymbol{m}} \tag{66}$$

with

$$\widetilde{\mathrm{cof}}\,\widetilde{\boldsymbol{F}} := \widetilde{J}\widetilde{\boldsymbol{f}}^{\mathrm{t}} \quad \text{and} \quad \widetilde{\mathrm{cof}}\,\widetilde{\boldsymbol{f}} := \widetilde{j}\widetilde{\boldsymbol{F}}^{\mathrm{t}}. \tag{67}$$

Again the definition of the curve cofactor $\widetilde{\mathrm{cof}}\{\bullet\}$ of the curve deformation gradient should not be confused with the cofactor of a rank deficient tensor as given in Proposition 1.1.5. of Šilhavý (1997).

Proof. With the explicit representations of the curve deformation gradients in Eq. (57) and the curve Jacobians in Eq. (61) the proof is trivial since $\widetilde{J}\widetilde{\boldsymbol{f}}^{\mathrm{t}} = \boldsymbol{t}\otimes\boldsymbol{T}$ and $\widetilde{j}\widetilde{\boldsymbol{F}}^{\mathrm{t}} = \boldsymbol{T}\otimes\boldsymbol{t}$ together with $\widetilde{\boldsymbol{M}}\|\boldsymbol{T}$ and $\widetilde{\boldsymbol{m}}\|\boldsymbol{t}$. □

Curve Piola Identity. The curve Piola identity gives an expression for the curve divergence of the curve cofactor of the curve deformation gradient

$$\widetilde{\mathrm{Div}}(\widetilde{\mathrm{cof}}\,\widetilde{\boldsymbol{F}}) = \widetilde{J}\,\mathsf{c}\,\boldsymbol{m} \quad \text{and} \quad \widetilde{\mathrm{div}}(\widetilde{\mathrm{cof}}\,\widetilde{\boldsymbol{f}}) = \widetilde{j}\,\mathsf{C}\,\boldsymbol{M}. \tag{68}$$

The curve Piola identity is the specialisation of the ordinary Piola identity to curves. Especially if the curve is flat in both configurations, i.e. $\mathsf{c} = 0$ and $\mathsf{C} = 0$, the similarity is obvious.

Proof. Since $\widetilde{\operatorname{cof}} \widetilde{\boldsymbol{F}} \cdot \boldsymbol{M} = \mathbf{0}$ and $\widetilde{\operatorname{cof}} \widetilde{\boldsymbol{f}} \cdot \boldsymbol{m} = \mathbf{0}$ the surface divergence theorem in Eq. (26) renders

$$\int_{\mathscr{C}_0'} \widetilde{\operatorname{Div}}(\widetilde{\operatorname{cof}} \widetilde{\boldsymbol{F}})\, \mathrm{d}L = \sum_{\mathscr{P}_0'} \widetilde{\operatorname{cof}} \widetilde{\boldsymbol{F}} \cdot \widetilde{\boldsymbol{M}} \quad \text{and} \quad \int_{\mathscr{C}_t'} \widetilde{\operatorname{div}}(\widetilde{\operatorname{cof}} \widetilde{\boldsymbol{f}})\, \mathrm{d}l = \sum_{\mathscr{P}_t'} \widetilde{\operatorname{cof}} \widetilde{\boldsymbol{f}} \cdot \widetilde{\boldsymbol{m}}. \tag{69}$$

With the curve Nanson formula in Eq. (66) and the point theorem in Eq. (27) the curve Piola identity is finally obtained from Eq. (69). □

Curve Piola Transforms. For curve quantities $\{\bullet\}$ related by curve Piola transforms $\{\bullet\} \mapsto \{\bullet\} \cdot \widetilde{\operatorname{cof}} \widetilde{\boldsymbol{F}}$ and $\{\bullet\} \mapsto \{\bullet\} \cdot \widetilde{\operatorname{cof}} \widetilde{\boldsymbol{f}}$ the curve Piola identity renders

$$\widetilde{\operatorname{Div}}(\{\bullet\} \cdot \widetilde{\operatorname{cof}} \widetilde{\boldsymbol{F}}) = \widetilde{J}[\widetilde{\operatorname{div}}(\{\bullet\}) + \mathsf{c}\, \{\bullet\} \cdot \boldsymbol{m}] \tag{70}$$

and

$$\widetilde{\operatorname{div}}(\{\bullet\} \cdot \widetilde{\operatorname{cof}} \widetilde{\boldsymbol{f}}) = \widetilde{j}[\widetilde{\operatorname{Div}}(\{\bullet\}) + \mathsf{C}\, \{\bullet\} \cdot \boldsymbol{M}].$$

Curve Piola transforms are the specialisation of the ordinary Piola transforms to curves. Especially if the curve is flat in both configurations, i.e. $\mathsf{c} = 0$ and $\mathsf{C} = 0$, or the $\{\bullet\}$ are tangent, i.e. $\{\bullet\} \cdot \boldsymbol{m} = 0$ or $\{\bullet\} \cdot \boldsymbol{M} = 0$, respectively, the similarity is obvious.

4. Deformational mechanics

The bulk potential energy density U_0 per material unit volume in $\mathscr{B}_0$ is composed of an internal and an external contribution W_0 and V_0 as

$$U_0 = W_0 + V_0 \quad \text{with } W_0 = W_0(\boldsymbol{F}; \boldsymbol{X}) \quad \text{and} \quad V_0 = V_0(\boldsymbol{\varphi}; \boldsymbol{X}). \tag{71}$$

Here the arguments of the energy densities in front of the semicolon depend on the unknown solution field $\boldsymbol{\varphi}$, whereas the other arguments denote the parametrisation in terms of the material position $\boldsymbol{X}$.

Likewise the surface potential energy density u_0 per material unit area in $\mathscr{S}_0$ consists of an internal and an external contribution w_0 and v_0 as

$$u_0 = w_0 + v_0 \quad \text{with } w_0 = w_0(\widehat{\boldsymbol{F}}; \boldsymbol{X}, \boldsymbol{N}) \quad \text{and} \quad v_0 = v_0(\boldsymbol{\varphi}, \boldsymbol{n}; \boldsymbol{X}, \boldsymbol{N}). \tag{72}$$

Here it deserves attention, that, in addition to the material position $\boldsymbol{X}$, in order to capture anisotropy, the parametrisation is also given in terms of the (outward) material surface normal $\boldsymbol{N}$. Moreover, for the sake of generality, we allow for a dependence of the external surface potential energy density, in addition to $\boldsymbol{\varphi}$, on the (outward) spatial surface normal $\boldsymbol{n}$ (think e.g. of follower loads).

Furthermore, the curve potential energy density u_0 per material unit length in $\mathscr{C}_0$ consists of an internal and an external contribution w_0 and v_0 as

$$\mathsf{u}_0 = \mathsf{w}_0 + \mathsf{v}_0 \quad \text{with } \mathsf{w}_0 = \mathsf{w}_0(\widetilde{\boldsymbol{F}}; \boldsymbol{X}, \boldsymbol{T}) \quad \text{and} \quad \mathsf{v}_0 = \mathsf{v}_0(\boldsymbol{\varphi}, \boldsymbol{t}; \boldsymbol{X}, \boldsymbol{T}). \tag{73}$$

Observe that, in addition to the material position $\boldsymbol{X}$, in order to capture anisotropy, the parametrisation is also given in terms of the material curve tangent $\boldsymbol{T}$. Moreover, for the sake of generality, we allow for a dependence of the external curve potential energy density, in addition to $\boldsymbol{\varphi}$, on the spatial curve tangent $\boldsymbol{t}$.

Finally, for the sake of completeness, we shall allow for a pointwise potential energy u in $\mathscr{P}_0$

$$\mathrm{u} = \mathrm{u}(\boldsymbol{\varphi}; \boldsymbol{X}). \tag{74}$$

In summary the total potential energy functional $I = I(\boldsymbol{\varphi})$ that we seek to minimise with respect to all admissible spatial variations $\mathrm{D}_\delta \boldsymbol{\varphi}$ at fixed material placement reads

$$I(\boldsymbol{\varphi}) := \int_{\mathscr{B}_0} U_0(\boldsymbol{\varphi}, \boldsymbol{F}; \boldsymbol{X})\, \mathrm{d}V + \int_{\mathscr{S}_0} u_0(\boldsymbol{\varphi}, \boldsymbol{n}, \widehat{\boldsymbol{F}}; \boldsymbol{X}, \boldsymbol{N})\, \mathrm{d}A + \int_{\mathscr{C}_0} \mathsf{u}_0(\boldsymbol{\varphi}, \boldsymbol{t}, \widetilde{\boldsymbol{F}}; \boldsymbol{X}, \boldsymbol{T})\, \mathrm{d}L + \sum_{\mathscr{P}_0} \mathrm{u}(\boldsymbol{\varphi}; \boldsymbol{X}). \tag{75}$$

Here $\mathscr{S}_0$, $\mathscr{C}_0$ and $\mathscr{P}_0$ contain the whole patchwork of surfaces, network of curves and set of points, respectively. Then the minimisation of the total potential energy functional $I(\boldsymbol{\varphi})$ renders the following:

Theorem. *In the bulk $\mathscr{B}_0$ the (localized) deformational force balance follows in standard form*

$$-[\operatorname{Div}\boldsymbol{P}+\boldsymbol{b}_0]=\boldsymbol{0} \quad \text{in } \mathscr{B}_0. \tag{76}$$

It is supplemented by the (localized) deformational force balance on the boundary surfaces in $\mathscr{S}_0=\partial\mathscr{B}_0$ that generalises the usual Neumann-type traction boundary conditions on $\partial\mathscr{B}_0$ as

$$\boldsymbol{P}\cdot\boldsymbol{N}^{\varsigma}-[\widehat{\operatorname{Div}}\,\widehat{\boldsymbol{P}}^{*}+\widehat{\boldsymbol{b}}_0]^{\varsigma}=\boldsymbol{0} \quad \text{on each } \mathscr{S}_0^{\varsigma} \quad \text{with } \widehat{\boldsymbol{P}}^{*}:=\widehat{\boldsymbol{P}}+\boldsymbol{n}\otimes\widehat{\boldsymbol{S}}_0. \tag{77}$$

The above statement is again supplemented by the (localized) deformational force balance that acts as a Neumann-type boundary condition on the boundary curves in $\mathscr{C}_0$ consisting of the boundaries to the surfaces in $\mathscr{S}_0$, whereby $\mathscr{S}_0^{\varsigma_\kappa}$ are the surfaces that intersect in the curve $\mathscr{C}_0^{\kappa}$

$$\sum_{\varsigma_\kappa}[\widehat{\boldsymbol{P}}^{*}\cdot\widehat{\boldsymbol{N}}]^{\varsigma_\kappa}-[\widetilde{\operatorname{Div}}\widetilde{\boldsymbol{P}}^{*}+\widetilde{\boldsymbol{b}}_0]^{\kappa}=\boldsymbol{0} \quad \text{on each } \mathscr{C}_0^{\kappa} \quad \text{with } \widetilde{\boldsymbol{P}}^{*}:=\widetilde{\boldsymbol{P}}+\widetilde{\boldsymbol{\pi}}_t\otimes\boldsymbol{T}. \tag{78}$$

The last statement is in turn supplemented by a Neumann-type boundary condition on the boundary points in $\mathscr{P}_0$ consisting of the boundaries to the curves in $\mathscr{C}_0$, whereby $\mathscr{C}_0^{\kappa_\pi}$ are the curves that intersect in the point $\mathscr{P}_0^{\pi}$

$$\sum_{\kappa_\pi}[\widetilde{\boldsymbol{P}}^{*}\cdot\widetilde{\boldsymbol{M}}]^{\kappa_\pi}-\bar{\boldsymbol{b}}^{\pi}=\boldsymbol{0} \quad \text{on each } \mathscr{P}_0^{\pi}. \tag{79}$$

Here the deformational stress in two-point description and the distributed force related to the bulk $\mathscr{B}_0$ are defined as usual as

$$\boldsymbol{P}:=\partial_{\boldsymbol{F}}U_0 \quad \text{and} \quad \boldsymbol{b}_0:=-\partial_{\boldsymbol{\varphi}}U_0. \tag{80}$$

Likewise, the deformational stress in two-point description and the distributed force (the traction) related to the surfaces in $\mathscr{S}_0$ (dimensions force per unit length and force per unit area, respectively) are defined as

$$\widehat{\boldsymbol{P}}:=\partial_{\widehat{\boldsymbol{F}}}u_0 \quad \text{and} \quad \widehat{\boldsymbol{b}}_0:=-\partial_{\boldsymbol{\varphi}}u_0. \tag{81}$$

Furthermore, the deformational stress in two-point description and the distributed force (the line load) related to the curves in $\mathscr{C}_0$ (dimensions force and force per unit length, respectively) are defined as

$$\widetilde{\boldsymbol{P}}:=\partial_{\widetilde{\boldsymbol{F}}}\mathsf{u}_0 \quad \text{and} \quad \widetilde{\boldsymbol{b}}_0:=-\partial_{\boldsymbol{\varphi}}\mathsf{u}_0. \tag{82}$$

Finally, the pointwise force related to the points in $\mathscr{P}_0$ (dimension force) is defined as

$$\bar{\boldsymbol{b}}:=-\partial_{\boldsymbol{\varphi}}\mathrm{u}. \tag{83}$$

As an additional quantity a deformational surface shear related to $\mathscr{S}_0$ is defined as

$$\widehat{\boldsymbol{S}}_0:=\widehat{\boldsymbol{\pi}}_t\cdot\widehat{\operatorname{cof}}\,\widehat{\boldsymbol{F}} \quad \text{with } \widehat{\boldsymbol{\pi}}_t:=-\partial_{\boldsymbol{n}}u_t\cdot\widehat{\boldsymbol{i}}. \tag{84}$$

The denomination surface shear was coined by Gurtin (2000) (although for the case of configurational mechanics, see below) and is motivated by the fact that the term $\boldsymbol{n}\otimes\widehat{\boldsymbol{S}}_0$ maps from the tangent space to the material surface $\mathscr{S}_0$ to the normal direction $\boldsymbol{n}$ of the spatial surface $\mathscr{S}_t$.

Likewise a deformational curve shear related to $\mathscr{C}_0$ is defined as

$$\widetilde{\boldsymbol{\pi}}_t:=\partial_{\boldsymbol{t}}\mathsf{u}_t\cdot\widetilde{\boldsymbol{i}}^{\perp}. \tag{85}$$

The denomination curve (junction) shear is credited to Simha and Bhattacharya (2000), (although for the case of configurational mechanics, see below) and is motivated by the fact that the term $\widetilde{\boldsymbol{\pi}}_t\otimes\boldsymbol{T}$ maps from the tangent space to the material curve $\mathscr{C}_0$ to the plane perpendicular to the tangent vector $\boldsymbol{t}$ of the spatial curve $\mathscr{C}_t$.

Proof. First, since (spatial) variation and integration at fixed material placement commute, the stationarity of the total potential energy functional $I(\boldsymbol{\varphi})$ in terms of its spatial variation $\mathrm{D}_\delta I$ is expressed as

$$\mathrm{D}_\delta I(\boldsymbol{\varphi}) = \int_{\mathscr{B}_0} \mathrm{D}_\delta U_0 \,\mathrm{d}V + \int_{\mathscr{S}_0} \mathrm{D}_\delta u_0 \,\mathrm{d}A + \int_{\mathscr{C}_0} \mathrm{D}_\delta \mathsf{u}_0 \,\mathrm{d}L + \sum_{\mathscr{P}_0} \mathrm{D}_\delta \mathsf{u} \doteq 0. \tag{86}$$

Second, the spatial variation of the bulk potential energy density renders

$$\mathrm{D}_\delta U_0 = \partial_{\boldsymbol{F}} U_0 : \mathrm{Grad}(\mathrm{D}_\delta \boldsymbol{\varphi}) + \partial_{\boldsymbol{\varphi}} \mathrm{U}_0 \cdot \mathrm{D}_\delta \boldsymbol{\varphi}.$$

Third, the spatial variation of surface potential energy density follows as

$$\mathrm{D}_\delta u_0 = [\partial_{\widehat{\boldsymbol{F}}} u_0 - \boldsymbol{n} \otimes \partial_{\boldsymbol{n}} u_t \cdot \widehat{\boldsymbol{i}} \cdot \widehat{\mathrm{cof}\,\boldsymbol{F}}] : \widehat{\mathrm{Grad}}(\mathrm{D}_\delta \boldsymbol{\varphi}) + \partial_{\boldsymbol{\varphi}} u_0 \cdot \mathrm{D}_\delta \boldsymbol{\varphi}.$$

Here we took into account Eq. (38) and considered that $\widehat{J}$ does not explicitly depend on $\boldsymbol{n}$, see Eq. (47.1).

Fourth, the spatial variation of curve potential energy density follows as

$$\mathrm{D}_\delta \mathsf{u}_0 = [\partial_{\widetilde{\boldsymbol{F}}} \mathsf{u}_0 + \partial_{\boldsymbol{t}} \mathsf{u}_t \cdot \widetilde{\boldsymbol{i}}^{\perp} \otimes \boldsymbol{T}] : \widetilde{\mathrm{Grad}}(\mathrm{D}_\delta \boldsymbol{\varphi}) + \partial_{\boldsymbol{\varphi}} \mathsf{u}_0 \cdot \mathrm{D}_\delta \boldsymbol{\varphi}.$$

Here we took into account Eq. (56) and considered that $\widetilde{J}$ does not explicitly depend on $\boldsymbol{t}$, see Eq. (64.1).

Next, using the definitions for the deformational stresses and distributed forces in Eqs. (80)–(85), applying integration by parts and the divergence and especially the surface and curve divergence theorems in Eqs. (12), (26) while observing that $\widehat{\boldsymbol{P}}^* \cdot \boldsymbol{N} = \boldsymbol{0}$ and $\widetilde{\boldsymbol{P}}^* \cdot \boldsymbol{M} = 0$, renders

$$\begin{aligned}
\mathrm{D}_\delta I(\boldsymbol{\varphi}) = &- \int_{\mathscr{B}_0} [\mathrm{Div}\,\boldsymbol{P} + \boldsymbol{b}_0] \cdot \mathrm{D}_\delta \boldsymbol{\varphi} \,\mathrm{d}V \\
&- \sum_{\varsigma} \int_{\mathscr{S}_0^{\varsigma}} \left[\widehat{\mathrm{Div}}\, \widehat{\boldsymbol{P}}^* + \widehat{\boldsymbol{b}}_0 - \boldsymbol{P} \cdot \boldsymbol{N} \right] \cdot \mathrm{D}_\delta \boldsymbol{\varphi} \,\mathrm{d}A \\
&- \sum_{\kappa} \int_{\mathscr{C}_0^{\kappa}} \left[\widetilde{\mathrm{Div}}\, \widetilde{\boldsymbol{P}}^* + \widetilde{\boldsymbol{b}}_0 - \sum_{\varsigma_\kappa} \widehat{\boldsymbol{P}}^* \cdot \widehat{\boldsymbol{N}} \right] \cdot \mathrm{D}_\delta \boldsymbol{\varphi} \,\mathrm{d}L \\
&- \sum_{\pi} \left[\bar{\boldsymbol{b}} - \sum_{\kappa_\pi} \widetilde{\boldsymbol{P}}^* \cdot \widetilde{\boldsymbol{M}} \right] \cdot \mathrm{D}_\delta \boldsymbol{\varphi} \doteq 0 \quad \forall \mathrm{D}_\delta \boldsymbol{\varphi}.
\end{aligned} \tag{87}$$

Finally, observing that the above expression has to vanish for all spatial variations of the spatial deformation map proves the theorem. □

Remark. The deformational surface shear $\widehat{\boldsymbol{S}}_0$, $\widehat{\boldsymbol{\pi}}_t$ is necessarily a tangential vector, i.e. $\widehat{\boldsymbol{S}}_0 \cdot \boldsymbol{N} = 0$, $\widehat{\boldsymbol{\pi}}_t \cdot \boldsymbol{n} = 0$. As a contrast, the deformational curve shear $\widetilde{\boldsymbol{\pi}}_t$ is necessarily perpendicular to the curve tangent $\boldsymbol{t}$, i.e. $\widetilde{\boldsymbol{\pi}}_t \cdot \boldsymbol{t} = 0$.

Remark. The contribution of the deformational surface shear $\widehat{\mathrm{Div}}(\boldsymbol{n} \otimes \widehat{\boldsymbol{S}}_0)$ in the (localized) deformational force balance at surfaces expands into $\boldsymbol{n}\, \widehat{\mathrm{Div}} \widehat{\boldsymbol{S}}_0 - \boldsymbol{k} \cdot \widehat{\boldsymbol{\pi}}_0$. Observe that the spatial description normal and tangential parts of this expression follow as $\widehat{\mathrm{Div}} \widehat{\boldsymbol{S}}_0$ and $-\boldsymbol{k} \cdot \widehat{\boldsymbol{\pi}}_0$. The contribution of the deformational curve shear $\widetilde{\mathrm{Div}}(\widetilde{\boldsymbol{\pi}}_t \otimes \boldsymbol{T})$ in the (localized) deformational force balance at curves reduces into $\partial_\Theta \widetilde{\boldsymbol{\pi}}_t = \widetilde{J} \partial_\theta \widetilde{\boldsymbol{\pi}}_t$, which appears to be a more common format for the curve divergence of a vector field.

Remark. In the above derivations we tacitly assumed that neither $\boldsymbol{P} \cdot \boldsymbol{N}$ nor $\widehat{\boldsymbol{P}}^* \cdot \widehat{\boldsymbol{N}}$ display a singularity when approaching a curve $\mathscr{C}_0^{\kappa}$ or a point $\mathscr{P}_0^{\pi}$, respectively. To consider singularities we have to follow and extend limiting arguments as put forth by Simha and Bhattacharya (1998,2000) which render the following additional contributions to Eqs. (78) and (79) respectively:

$$\widetilde{\boldsymbol{b}}_0^{s\kappa} := \lim_{r \to 0} \int_{\partial \mathscr{D}_0^{\kappa} \cap \mathscr{B}_0} \boldsymbol{P} \cdot \boldsymbol{N} \,\mathrm{d}\mathscr{L}.$$

$$\bar{\boldsymbol{b}}^{s\pi} := \lim_{r\to 0}\int_{\partial\mathscr{B}_0^\pi\cap\mathscr{B}_0} \boldsymbol{P}\cdot\boldsymbol{N}\,\mathrm{d}\mathscr{A} + \sum_{\varsigma_\pi}\lim_{r\to 0}\int_{\partial\mathscr{B}_0^\pi\cap\mathscr{S}_0^{\varsigma_\pi}} \widehat{\boldsymbol{P}}^*\cdot\widehat{\boldsymbol{N}}\,\mathrm{d}\mathscr{L}.$$

Here $\mathscr{D}_0^\kappa$ denotes a disk with radius r in the plane perpendicular to the tangent vector at arclength Θ of curve $\mathscr{C}_0^\kappa$ and centered at $\mathscr{C}_0^\kappa$, moreover $\mathscr{B}_0^\pi$ denotes a ball with radius r centered at $\mathscr{P}_0^\pi$. To obtain the above result the minimisation of the energy functional $I(\boldsymbol{\varphi})$ has to be performed on $\mathscr{B}_0\backslash[\cup\mathscr{T}_0^\kappa\cup\mathscr{B}_0^\pi]$ and $\mathscr{S}_0\backslash[\cup\mathscr{B}_0^\pi]$ and taking the limit $r\to 0$, whereby $\mathscr{T}_0^\kappa$ is a tube generated by the disks $\mathscr{D}_0^\kappa$ along the curves $\mathscr{C}_0^\kappa$. These contributions become critical if singularities exist, nevertheless, for the simplicity of exposition, we shall not explicitly indicate those in the sequel, keeping in mind how and where to add terms if necessary.

The deformational balance equations in the above theorem are formulated in terms of deformational two-point description stresses in the bulk, on the surfaces and on the curves. An equivalent formulation that relies on deformational spatial description stresses in the bulk, the surfaces and the curves is given in the following:

Theorem. *In the bulk $\mathscr{B}_t$ the (localized) deformational force balance takes the standard form*

$$-[\operatorname{div}\boldsymbol{\sigma}+\boldsymbol{b}_t]=\boldsymbol{0}\quad in\ \mathscr{B}_t. \tag{88}$$

It is supplemented by the (localized) deformational force balance on the boundary surfaces in $\mathscr{S}_t$ as

$$\boldsymbol{\sigma}\cdot\boldsymbol{n}^\varsigma-[\widehat{\operatorname{div}}\widehat{\boldsymbol{\sigma}}^*+\widehat{\boldsymbol{b}}_t]^\varsigma=\boldsymbol{0}\quad on\ each\ \mathscr{S}_t^\varsigma\quad with\ \widehat{\boldsymbol{\sigma}}^*:=\widehat{\boldsymbol{\sigma}}+\boldsymbol{n}\otimes\widehat{\boldsymbol{\pi}}_t. \tag{89}$$

The above statement is again supplemented by the (localized) deformational force balance that acts as a Neumann-type boundary condition on the boundary curves in $\mathscr{C}_t$ as

$$\sum_{\varsigma_\kappa}[\widehat{\boldsymbol{\sigma}}^*\cdot\widehat{\boldsymbol{n}}]^{\varsigma_\kappa}-[\widetilde{\operatorname{div}}\widetilde{\boldsymbol{\sigma}}^*+\widetilde{\boldsymbol{b}}_t]^\kappa=\boldsymbol{0}\quad on\ each\ \mathscr{C}_t^\kappa\quad with\ \widetilde{\boldsymbol{\sigma}}^*:=\widetilde{\boldsymbol{\sigma}}+\widetilde{\boldsymbol{\pi}}_t\otimes\boldsymbol{t}. \tag{90}$$

The last statement is in turn supplemented by a Neumann-type boundary condition on the boundary points in $\mathscr{P}_t$ as

$$\sum_{\kappa_\pi}[\widetilde{\boldsymbol{\sigma}}^*\cdot\widetilde{\boldsymbol{m}}]^{\kappa_\pi}-\bar{\boldsymbol{b}}^\pi=\boldsymbol{0}\quad on\ each\ \mathscr{P}_t^\pi. \tag{91}$$

Here the deformational stress in spatial description and the distributed force related to the bulk $\mathscr{B}_t$ follow as

$$\boldsymbol{\sigma}:=U_t\boldsymbol{i}+\partial_{\boldsymbol{F}}U_t\cdot\boldsymbol{F}^{\mathrm{t}}\quad and\quad \boldsymbol{b}_t:=-\partial_{\boldsymbol{\varphi}}U_t. \tag{92}$$

Likewise, the deformational stress in spatial description and the distributed force related to the surfaces in $\mathscr{S}_t$ are given by

$$\widehat{\boldsymbol{\sigma}}:=u_t\widehat{\boldsymbol{i}}+\partial_{\widehat{\boldsymbol{F}}}u_t\cdot\widehat{\boldsymbol{F}}^{\mathrm{t}}\quad and\quad \widehat{\boldsymbol{b}}_t:=-\partial_{\boldsymbol{\varphi}}u_t. \tag{93}$$

Furthermore, the deformational stress in spatial description and the distributed force related to the curves in $\mathscr{C}_t$ are defined as

$$\widetilde{\boldsymbol{\sigma}}:=\mathsf{u}_t\widetilde{\boldsymbol{i}}+\partial_{\widetilde{\boldsymbol{F}}}\mathsf{u}_t\cdot\widetilde{\boldsymbol{F}}^{\mathrm{t}}\quad and\quad \widetilde{\boldsymbol{b}}_t:=-\partial_{\boldsymbol{\varphi}}\mathsf{u}_t. \tag{94}$$

The deformational surface and curve shear $\widehat{\boldsymbol{\pi}}_t$ and $\widetilde{\boldsymbol{\pi}}_t$ in spatial description related to $\mathscr{S}_t$ and $\mathscr{C}_t$ as well as the pointwise force $\bar{\boldsymbol{b}}$ related to $\mathscr{P}_t$ have already been defined in Eqs. (84), (85) *and* (83).

Proof. Since $U_0=JU_t$, the spatial variation of the bulk potential energy density follows as

$$j\,\mathrm{D}_\delta[JU_t]=[U_t\boldsymbol{i}+\partial_{\boldsymbol{F}}U_t\cdot\boldsymbol{F}^{\mathrm{t}}]:\operatorname{grad}(\mathrm{D}_\delta\boldsymbol{\varphi})+\partial_{\boldsymbol{\varphi}}U_t\cdot\,\mathrm{D}_\delta\boldsymbol{\varphi}.$$

Likewise, since $u_t=\widehat{J}u_t$, the spatial variation of the surface potential energy density follows with Eq. (47.1) as

$$\widehat{j}\,\mathrm{D}_\delta[\widehat{J}u_t]=[u_t\widehat{\boldsymbol{i}}+\partial_{\widehat{\boldsymbol{F}}}u_t\cdot\widehat{\boldsymbol{F}}^{\mathrm{t}}-\boldsymbol{n}\otimes\partial_{\boldsymbol{n}}u_t\cdot\widehat{\boldsymbol{i}}]:\widehat{\operatorname{grad}}(\mathrm{D}_\delta\boldsymbol{\varphi})+\partial_{\boldsymbol{\varphi}}u_t\cdot\,\mathrm{D}_\delta\boldsymbol{\varphi}.$$

Finally, since $\mathsf{u}_t=\widetilde{J}\mathsf{u}_t$, the spatial variation of the curve potential energy density follows with Eq. (64.1) as

$$\widetilde{j}\,\mathrm{D}_\delta[\widetilde{J}\mathsf{u}_t]=[\mathsf{u}_t\widetilde{\boldsymbol{i}}+\partial_{\widetilde{\boldsymbol{F}}}\mathsf{u}_t\cdot\widetilde{\boldsymbol{F}}^{\mathrm{t}}+\partial_{\boldsymbol{t}}\mathsf{u}_t\cdot\widetilde{\boldsymbol{i}}^{\perp}\otimes\boldsymbol{t}]:\widetilde{\operatorname{grad}}(\mathrm{D}_\delta\boldsymbol{\varphi})+\partial_{\boldsymbol{\varphi}}\mathsf{u}_t\cdot\,\mathrm{D}_\delta\boldsymbol{\varphi}.$$

Using further the definitions for the deformational stresses and distributed forces in Eqs. (92)–(94), (83)–(85), applying integration by parts and the divergence and especially the surface and curve divergence theorems in Eqs. (12), (26) while observing that $\widehat{\boldsymbol{\sigma}}^* \cdot \boldsymbol{n} = \boldsymbol{0}$ and $\widetilde{\boldsymbol{\sigma}}^* \cdot \boldsymbol{m} = 0$, renders

$$\begin{aligned} \mathrm{D}_\delta I(\boldsymbol{\varphi}) = & -\int_{\mathscr{B}_t} [\operatorname{div}\boldsymbol{\sigma} + \boldsymbol{b}_t] \cdot \mathrm{D}_\delta \boldsymbol{\varphi} \, \mathrm{d}v \\ & -\sum_{\varsigma} \int_{\mathscr{S}_t^\varsigma} \left[\widehat{\operatorname{div}} \widehat{\boldsymbol{\sigma}}^* + \widehat{\boldsymbol{b}}_t - \boldsymbol{\sigma} \cdot \boldsymbol{n} \right] \cdot \mathrm{D}_\delta \boldsymbol{\varphi} \, \mathrm{d}a \\ & -\sum_{\kappa} \int_{\mathscr{C}_t^\kappa} \left[\widetilde{\operatorname{div}} \widetilde{\boldsymbol{\sigma}}^* + \widetilde{\boldsymbol{b}}_t - \sum_{\varsigma_\kappa} \widehat{\boldsymbol{\sigma}}^* \cdot \widehat{\boldsymbol{n}} \right] \cdot \mathrm{D}_\delta \boldsymbol{\varphi} \, \mathrm{d}l \\ & -\sum_{\pi} \left[\bar{\boldsymbol{b}} - \sum_{\kappa_\pi} \widetilde{\boldsymbol{\sigma}}^* \cdot \widetilde{\boldsymbol{m}} \right] \cdot \mathrm{D}_\delta \boldsymbol{\varphi} \doteq 0 \quad \forall\, \mathrm{D}_\delta \boldsymbol{\varphi}. \end{aligned} \tag{95}$$

Finally, observing that the above expression has to vanish for all spatial variations of the spatial deformation map proves the theorem. □

Remark. The mixed-variant deformational two-point and spatial description stresses in the surfaces are related by surface pull-back/push-forward operations that are formally similar to the well-known pull-back/push-forward operations of the stresses in the bulk

$$\widehat{\boldsymbol{P}} = \widehat{\boldsymbol{\sigma}} \cdot \widehat{\operatorname{cof}}\, \widehat{\boldsymbol{F}} = \widehat{J} \widehat{\sigma}_\alpha{}^\beta \boldsymbol{a}^\alpha \otimes \boldsymbol{A}_\beta \quad \text{and} \quad \widehat{\boldsymbol{\sigma}} = \widehat{\boldsymbol{P}} \cdot \widehat{\operatorname{cof}}\, \widehat{\boldsymbol{f}} = \widehat{\sigma}_\alpha{}^\beta \boldsymbol{a}^\alpha \otimes \boldsymbol{a}_\beta. \tag{96}$$

Thus, the deformational surface Piola and Cauchy stresses $\widehat{\boldsymbol{P}}$ and $\widehat{\boldsymbol{\sigma}}$ are related by Piola transformations and, according to Eq. (54) and due to being tangential, satisfy $\widehat{\operatorname{Div}}\, \widehat{\boldsymbol{P}} = \widehat{J}\, \widehat{\operatorname{div}}\, \widehat{\boldsymbol{\sigma}}$. The corresponding surface pull-back/push-forward of the deformational surface shear, resulting in $\widehat{\operatorname{Div}}\, \widehat{\boldsymbol{S}}_0 = \widehat{J}\, \widehat{\operatorname{div}}\, \widehat{\boldsymbol{\pi}}_t$, reads

$$\widehat{\boldsymbol{S}}_0 = \widehat{\boldsymbol{\pi}}_t \cdot \widehat{\operatorname{cof}}\, \widehat{\boldsymbol{F}} = \widehat{\pi}_0^\beta \boldsymbol{A}_\beta \quad \text{and} \quad \widehat{\boldsymbol{\pi}}_t = \widehat{\boldsymbol{S}}_0 \cdot \widehat{\operatorname{cof}}\, \widehat{\boldsymbol{f}} = \widehat{\pi}_t^\beta \boldsymbol{a}_\beta. \tag{97}$$

Likewise, the mixed-variant deformational two-point and spatial description stresses in the curves are related by curve pull-back/push-forward operations

$$\widetilde{\boldsymbol{P}} = \widetilde{\boldsymbol{\sigma}} \cdot \widetilde{\operatorname{cof}}\, \widetilde{\boldsymbol{F}} = \widetilde{\sigma}\, \boldsymbol{t} \otimes \boldsymbol{T} \quad \text{and} \quad \widetilde{\boldsymbol{\sigma}} = \widetilde{\boldsymbol{P}} \cdot \widetilde{\operatorname{cof}}\, \widetilde{\boldsymbol{f}} = \widetilde{\sigma}\, \boldsymbol{t} \otimes \boldsymbol{t}. \tag{98}$$

Thus, the deformational curve Piola and Cauchy stresses $\widetilde{\boldsymbol{P}}$ and $\widetilde{\boldsymbol{\sigma}}$ are related by Piola transformations and, according to Eq. (70) and due to being tangential, satisfy $\widetilde{\operatorname{Div}} \widetilde{\boldsymbol{P}} = \widetilde{J}\, \widetilde{\operatorname{div}}\, \widetilde{\boldsymbol{\sigma}}$.

5. Configurational mechanics

Within the setting of configurational mechanics the role of fields and parametrisation are reversed with respect to the setting of deformational mechanics (e.g. $\boldsymbol{\varphi}(\boldsymbol{X}) \to \boldsymbol{x}$ and $\boldsymbol{X} \to \boldsymbol{\Phi}(\boldsymbol{x})$). Moreover, since we shall consider material variations at fixed spatial placements, it proves convenient to express the various potential energy densities with respect to the spatial rather than the material unit volumes in $\mathscr{B}_t$, unit areas in $\mathscr{S}_t$ and unit length in $\mathscr{C}_t$.

The bulk potential energy density U_t or rather its internal and external contributions W_t and V_t have arguments

$$U_t = W_t + V_t \quad \text{with } W_t = W_t(\boldsymbol{F}, \boldsymbol{\Phi}) \quad \text{and} \quad V_t = V_t(\boldsymbol{\Phi}; \boldsymbol{x}). \tag{99}$$

Now the arguments of the energy densities in front of the semicolon depend on the unknown solution field $\boldsymbol{\Phi}$ (i.e. the material placement), whereas the other arguments denote the parametrisation in terms of the spatial position $\boldsymbol{x}$. Likewise, the surface potential energy density u_t in terms of the internal and external contributions w_t and v_t reads

$$u_t = w_t + v_t \quad \text{with } w_t = w_t(\widehat{\boldsymbol{F}}, \boldsymbol{\Phi}, \boldsymbol{N}) \quad \text{and} \quad v_t = v_t(\boldsymbol{\Phi}, \boldsymbol{N}; \boldsymbol{x}, \boldsymbol{n}). \tag{100}$$

Furthermore, the curve potential energy density u_t in terms of the internal and external contributions w_t and v_t is given as

$$\mathsf{u}_t = \mathsf{w}_t + \mathsf{v}_t \quad \text{with } \mathsf{w}_t = \mathsf{w}_t(\widetilde{\boldsymbol{F}}, \boldsymbol{\Phi}, \boldsymbol{T}) \quad \text{and} \quad \mathsf{v}_t = \mathsf{v}_t(\boldsymbol{\Phi}, \boldsymbol{T}; \boldsymbol{x}, \boldsymbol{t}). \tag{101}$$

Finally, the pointwise potential energy u in $\mathscr{P}_t$ also changes fields and parametrisation

$$\mathrm{u} = \mathrm{u}(\boldsymbol{\Phi}; \boldsymbol{x}). \tag{102}$$

In summary the total potential energy functional $I = I(\boldsymbol{\Phi})$ that we shall analyse in the sequel with respect to its changes under admissible material variations $\mathrm{d}_\delta\boldsymbol{\Phi}$ reads

$$I(\boldsymbol{\Phi}) := \int_{\mathscr{B}_t} U_t(\boldsymbol{\Phi}, \boldsymbol{F}; \boldsymbol{x})\,\mathrm{d}v + \int_{\mathscr{S}_t} u_t(\boldsymbol{\Phi}, \boldsymbol{N}, \widehat{\boldsymbol{F}}; \boldsymbol{x}, \boldsymbol{n})\,\mathrm{d}a + \int_{\mathscr{C}_t} \mathsf{u}_t(\boldsymbol{\Phi}, \boldsymbol{T}, \widetilde{\boldsymbol{F}}; \boldsymbol{x}, \boldsymbol{t})\,\mathrm{d}l + \sum_{\mathscr{P}_t} \mathrm{u}(\boldsymbol{\Phi}; \boldsymbol{x}). \tag{103}$$

It is now important to recognise that taking a material variation $\mathrm{d}_\delta\{\bullet\}$ of the total potential energy functional at fixed spatial placement only leads to a stationary point $\mathrm{d}_\delta I = 0$ for the case of configurational equilibrium. Nevertheless, in general cases a material variation $\mathrm{d}_\delta I$ renders a change of the total potential energy functional

$$\mathrm{d}_\delta I(\boldsymbol{\Phi}) =: \mathscr{R} \leqslant 0. \tag{104}$$

The inequality is a reminder of the second law, since changes in configuration $\mathrm{d}_\delta\boldsymbol{\Phi}$ are only admissible if potential energy is released, compare the classical arguments related to the possible extension of cracks. In general this virtual energy release could be dissipated by other physical processes like e.g. the creation of new crack surfaces, the material motion of defects etc. The key idea of configurational mechanics is that configurational forces act on all kinds of defects (vacancies or inclusions, cracks, interfaces or phase boundaries and the like) and capture the energetic changes that go along with material motions of the defects relative to the ambient material, i.e. configurational changes. Here we shall for simplicity consider possible continuously distributed 'defects',[4] thus only distributed configurational forces $\boldsymbol{B}_t^d$ (per unit volume), $\widehat{\boldsymbol{B}}_t^d$ (per unit area), $\widetilde{\boldsymbol{B}}_t^d$ (per unit length) and the pointwise configurational force $\bar{\boldsymbol{B}}^d$ related to $\mathscr{B}_t$, $\mathscr{S}_t$, $\mathscr{C}_t$ and $\mathscr{P}_t$,respectively, appear and are power conjugate to configurational variations $\mathrm{d}_\delta\boldsymbol{\Phi}$

$$\mathscr{R} := \int_{\mathscr{B}_t} \boldsymbol{B}_t^d \cdot \mathrm{d}_\delta\boldsymbol{\Phi}\,\mathrm{d}v + \int_{\mathscr{S}_t} \widehat{\boldsymbol{B}}_t^d \cdot \mathrm{d}_\delta\boldsymbol{\Phi}\,\mathrm{d}a + \int_{\mathscr{C}_t} \widetilde{\boldsymbol{B}}_t^d \cdot \mathrm{d}_\delta\boldsymbol{\Phi}\,\mathrm{d}l + \sum_{\mathscr{P}_t} \bar{\boldsymbol{B}}^d \cdot \mathrm{d}_\delta\boldsymbol{\Phi}. \tag{105}$$

In summary, the configurational forces $\boldsymbol{B}_t^d$, $\widehat{\boldsymbol{B}}_t^d$, $\widetilde{\boldsymbol{B}}_t^d$ and $\bar{\boldsymbol{B}}^d$ introduced above come as definitions in order to capture the energetic changes associated with configurational variations.

Finally, the exploitation of the energy release statement in Eq. (104) for the total potential energy functional $I(\boldsymbol{\Phi})$ together with the definition in Eq. (105) renders the following:

Theorem. *In the bulk $\mathscr{B}_t$ the (localized) configurational force balance follows as*

$$-[\operatorname{div}\boldsymbol{p} + \boldsymbol{B}_t] := \boldsymbol{B}_t^d \quad \text{in } \mathscr{B}_t. \tag{106}$$

It is supplemented by the (localized) configurational force balance on the boundary surfaces in $\mathscr{S}_t$ as

$$\boldsymbol{p}\cdot\boldsymbol{n}^\varsigma - [\widehat{\operatorname{div}}\widehat{\boldsymbol{p}}^* + \widehat{\boldsymbol{B}}_t]^\varsigma =: \widehat{\boldsymbol{B}}_t^{d\varsigma} \quad \text{on each } \mathscr{S}_t^\varsigma \quad \text{with } \widehat{\boldsymbol{p}}^* := \widehat{\boldsymbol{p}} + \boldsymbol{N}\otimes\widehat{\boldsymbol{s}}_t. \tag{107}$$

The above statement is again supplemented by the (localized) configurational force balance that acts as a Neumann-type boundary condition on the boundary curves in $\mathscr{C}_t$ as

$$\sum_{\varsigma_\kappa}[\widehat{\boldsymbol{p}}^*\cdot\widehat{\boldsymbol{n}}]^{\varsigma_\kappa} - [\widetilde{\operatorname{div}}\widetilde{\boldsymbol{p}}^* + \widetilde{\boldsymbol{B}}_t]^\kappa := \widetilde{\boldsymbol{B}}_t^{d\kappa} \quad \text{on each } \mathscr{C}_t^\kappa \quad \text{with } \widetilde{\boldsymbol{p}}^* := \widetilde{\boldsymbol{p}} + \widetilde{\pi}_0\otimes\boldsymbol{t}. \tag{108}$$

[4]The case of discrete defects or singularities in $\mathscr{B}_t$, $\mathscr{S}_t$ or $\mathscr{C}_t$ can be treated in the same fashion by expressing $\boldsymbol{B}_t^d$, $\widehat{\boldsymbol{B}}_t^d$ and $\widetilde{\boldsymbol{B}}_t^d$ in terms of appropriate Dirac distributions. Moreover, we have to follow the cut-out and limiting procedure sketched previously when analysing the spatial variation of the energy functional.

The last statement is in turn supplemented by a Neumann-type boundary condition on the boundary points in $\mathscr{P}_0$ as

$$\sum_{\kappa_\pi}[\widetilde{\boldsymbol{p}}^* \cdot \widetilde{\boldsymbol{m}}]^{\kappa_\pi} - \bar{\boldsymbol{B}}^\pi \coloneqq \bar{\boldsymbol{B}}^{d\pi} \quad \text{on each } \mathscr{P}_t^\pi. \tag{109}$$

Here the configurational stress in two-point description and the distributed force related to the bulk $\mathscr{B}_t$ are defined as

$$\boldsymbol{p} \coloneqq -\boldsymbol{F}^{\mathrm{t}} \cdot \partial_{\boldsymbol{F}} U_{\mathrm{t}} \cdot \boldsymbol{F}^{\mathrm{t}} \quad \text{and} \quad \boldsymbol{B}_t \coloneqq -\partial_{\boldsymbol{\Phi}} U_t. \tag{110}$$

Likewise, the configurational stress in two-point description and the distributed force related to the surfaces in $\mathscr{S}_t$ are defined as

$$\widehat{\boldsymbol{p}} \coloneqq -\widehat{\boldsymbol{F}}^{\mathrm{t}} \cdot \partial_{\widehat{\boldsymbol{F}}} u_t \cdot \widehat{\boldsymbol{F}}^{\mathrm{t}} \quad \text{and} \quad \widehat{\boldsymbol{B}}_t \coloneqq -\partial_{\boldsymbol{\Phi}} u_t. \tag{111}$$

Furthermore, the configurational stress in two-point description and the distributed force related to the curves in $\mathscr{C}_t$ are defined as

$$\widetilde{\boldsymbol{p}} \coloneqq -\widetilde{\boldsymbol{F}}^{\mathrm{t}} \cdot \partial_{\widetilde{\boldsymbol{F}}} \mathsf{u}_t \cdot \widetilde{\boldsymbol{F}}^{\mathrm{t}} \quad \text{and} \quad \widetilde{\boldsymbol{B}}_t \coloneqq -\partial_{\boldsymbol{\Phi}} \mathsf{u}_t. \tag{112}$$

Finally, the pointwise configurational force related to the points in $\mathscr{P}_t$ is defined as

$$\bar{\boldsymbol{B}} \coloneqq -\partial_{\boldsymbol{\Phi}} \mathrm{u}. \tag{113}$$

As an additional quantity a configurational surface shear related to $\mathscr{S}_t$ is defined as

$$\widehat{\boldsymbol{s}}_t \coloneqq \widehat{\boldsymbol{\Pi}}_0 \cdot \widehat{\operatorname{cof}} \widehat{\boldsymbol{f}} \quad \text{with } \widehat{\boldsymbol{\Pi}}_0 \coloneqq -\partial_{\boldsymbol{N}} u_0 \cdot \widehat{\boldsymbol{I}}. \tag{114}$$

Likewise, the configurational curve shear related to $\mathscr{C}_0$ is defined as

$$\widetilde{\boldsymbol{\Pi}}_0 \coloneqq \partial_{\boldsymbol{T}} \mathsf{u}_0 \cdot \widetilde{\boldsymbol{I}}^{\perp}. \tag{115}$$

As mentioned above, the terminology surface shear goes back to, Gurtin (2000), whereas the terminology curve (junction) shear can be credited to Simha and Bhattacharya (2000).

Proof. First, since (material) variation and integration at fixed spatial placement commute, the material variation of the total potential energy functional $I(\boldsymbol{\Phi})$ is expressed as

$$\mathrm{d}_\delta I(\boldsymbol{\Phi}) = \int_{\mathscr{B}_t} \mathrm{d}_\delta U_t \,\mathrm{d}v + \int_{\mathscr{S}_t} \mathrm{d}_\delta u_t \,\mathrm{d}a + \int_{\mathscr{C}_t} \mathrm{d}_\delta \mathsf{u}_t \,\mathrm{d}l + \sum_{\mathscr{P}_t} \mathrm{d}_\delta \mathrm{u} \coloneqq \mathscr{R}. \tag{116}$$

Second, with $\mathrm{d}_\delta \boldsymbol{F} = -\boldsymbol{F} \cdot \mathrm{d}_\delta \boldsymbol{f} \cdot \boldsymbol{F}$ the material variation of the bulk potential energy density renders

$$\mathrm{d}_\delta U_t = -[\boldsymbol{F}^{\mathrm{t}} \cdot \partial_{\boldsymbol{F}} U_t \cdot \boldsymbol{F}^{\mathrm{t}}] : \operatorname{grad}(\mathrm{d}_\delta \boldsymbol{\Phi}) + \partial_{\boldsymbol{\Phi}} U_t \cdot \mathrm{d}_\delta \boldsymbol{\Phi}.$$

Third, with Eq. (42) the material variation of the surface potential energy density follows as

$$\mathrm{d}_\delta u_t = -[\widehat{\boldsymbol{F}}^{\mathrm{t}} \cdot \partial_{\widehat{\boldsymbol{F}}} u_t \cdot \widehat{\boldsymbol{F}}^{\mathrm{t}} + \boldsymbol{N} \otimes \partial_{\boldsymbol{N}} u_0 \cdot \widehat{\boldsymbol{I}} \cdot \widehat{\operatorname{cof}} \widehat{\boldsymbol{f}}] : \widehat{\operatorname{grad}}(\mathrm{d}_\delta \boldsymbol{\Phi}) + \partial_{\boldsymbol{\Phi}} u_t \cdot \mathrm{d}_\delta \boldsymbol{\Phi}.$$

Here we took into account Eq. (38) and considered that $\hat{j}$ does not explicitly depend on $\boldsymbol{N}$, see Eq. (47).
Fourth, with Eq. (60) the material variation of the curve potential energy density follows as

$$\mathrm{d}_\delta \mathsf{u}_t = -[\widetilde{\boldsymbol{F}}^{\mathrm{t}} \cdot \partial_{\widetilde{\boldsymbol{F}}} \mathsf{u}_t \cdot \widetilde{\boldsymbol{F}}^{\mathrm{t}} - \partial_{\boldsymbol{T}} \mathsf{u}_0 \cdot \widetilde{\boldsymbol{I}}^{\perp} \otimes \boldsymbol{t}] : \widetilde{\operatorname{grad}}(\mathrm{d}_\delta \boldsymbol{\Phi}) + \partial_{\boldsymbol{\Phi}} \mathsf{u}_t \cdot \mathrm{d}_\delta \boldsymbol{\Phi}.$$

Here we took into account Eq. (56) and considered that $\tilde{j}$ does not explicitly depend on $\boldsymbol{T}$, see Eq. (64.2).

Next, using the definitions for the configurational stresses and distributed forces in Eqs. (110)–(115), applying integration by parts and the divergence and especially the surface and curve divergence theorems in Eqs. (12), (26) while observing that $\widehat{\boldsymbol{p}}^* \cdot \boldsymbol{n} = \boldsymbol{0}$ and $\widetilde{\boldsymbol{p}}^* \cdot \boldsymbol{m} = 0$, renders

$$\begin{aligned} \mathrm{d}_\delta I(\boldsymbol{\Phi}) = & -\int_{\mathscr{B}_t} [\operatorname{div} \boldsymbol{p} + \boldsymbol{B}_t] \cdot \mathrm{d}_\delta \boldsymbol{\Phi} \, \mathrm{d}v \\ & - \sum_{\varsigma} \int_{\mathscr{S}_t^\varsigma} [\widehat{\operatorname{div}} \widehat{\boldsymbol{p}}^* + \widehat{\boldsymbol{B}}_t - \boldsymbol{p} \cdot \boldsymbol{n}] \cdot \mathrm{d}_\delta \boldsymbol{\Phi} \, \mathrm{d}a \\ & - \sum_{\kappa} \int_{\mathscr{C}_t^\kappa} \left[\widetilde{\operatorname{div}} \widetilde{\boldsymbol{p}}^* + \widetilde{\boldsymbol{B}}_t - \sum_{\varsigma_\kappa} \widehat{\boldsymbol{p}}^* \cdot \widehat{\boldsymbol{n}} \right] \cdot \mathrm{d}_\delta \boldsymbol{\Phi} \, \mathrm{d}l \\ & - \sum_{\pi} \left[\bar{\boldsymbol{B}} - \sum_{\kappa_\pi} \widetilde{\boldsymbol{p}}^* \cdot \widetilde{\boldsymbol{m}} \right] \cdot \mathrm{d}_\delta \boldsymbol{\Phi} =: \mathscr{R} \quad \forall \mathrm{d}_\delta \boldsymbol{\Phi}. \end{aligned} \tag{117}$$

Finally, observing that the above statement has to be satisfied for all material variations of the material deformation map proves the theorem. □

Remark. The configurational surface shear $\widehat{\boldsymbol{s}}_t$, $\widehat{\boldsymbol{\Pi}}_0$ is necessarily a tangential vector, i.e. $\widehat{\boldsymbol{s}}_t \cdot \boldsymbol{n} = 0$, $\widehat{\boldsymbol{\Pi}}_0 \cdot \boldsymbol{N} = 0$. The configurational curve shear $\widetilde{\boldsymbol{\Pi}}_0$, on the other hand, is necessarily perpendicular to the curve tangent $\boldsymbol{T}$, i.e. $\widetilde{\boldsymbol{\Pi}}_0 \cdot \boldsymbol{T} = 0$.

Remark. The contribution of the configurational surface shear $\widehat{\operatorname{div}}(\boldsymbol{N} \otimes \widehat{\boldsymbol{s}}_t)$ in the (localized) configurational force balance at surfaces expands into $\boldsymbol{N}\, \widehat{\operatorname{div}} \widehat{\boldsymbol{s}}_t - \boldsymbol{K} \cdot \widehat{\boldsymbol{\Pi}}_t$. Observe that the material description normal and tangential parts of this expression follow as $\widehat{\operatorname{div}} \widehat{\boldsymbol{s}}_t$ and $-\boldsymbol{K} \cdot \widehat{\boldsymbol{\Pi}}_t$. The contribution of the configurational curve shear $\widetilde{\operatorname{div}}(\widetilde{\boldsymbol{\Pi}}_0 \otimes \boldsymbol{t})$ in the (localized) configurational force balance at curves reduces into $\partial_\theta \widetilde{\boldsymbol{\Pi}}_0 = \widetilde{j} \partial_\Theta \widetilde{\boldsymbol{\Pi}}_0$,which is the common format for the curve divergence of a vector field.

The configurational balance equations in the above theorem are formulated in terms of configurational two-point description stresses in the bulk, on the surfaces and on the curves. An equivalent formulation that relies on configurational material description stresses in the bulk, the surfaces and the curves is given in the following:

Theorem. *In the bulk $\mathscr{B}_0$ the (localized) configurational force balance takes the form*

$$-[\operatorname{Div} \boldsymbol{\Sigma} + \boldsymbol{B}_0] =: \boldsymbol{B}_0^d \quad \textit{in } \mathscr{B}_0. \tag{118}$$

It is supplemented by the (localized) configurational force balance on the boundary surfaces in $\mathscr{S}_0$ as

$$\boldsymbol{\Sigma} \cdot \boldsymbol{N}^\varsigma - [\widehat{\operatorname{Div}}\, \widehat{\boldsymbol{\Sigma}}^* + \widehat{\boldsymbol{B}}_0]^\varsigma =: \widehat{\boldsymbol{B}}_0^{d\varsigma} \quad \textit{on each } \mathscr{S}_0^\varsigma \quad \textit{with } \widehat{\boldsymbol{\Sigma}}^* := \widehat{\boldsymbol{\Sigma}} + \boldsymbol{N} \otimes \widehat{\boldsymbol{\Pi}}_0. \tag{119}$$

The above statement is again supplemented by the (localized) configurational force balance that acts as a Neumann-type boundary condition on the boundary curves in $\mathscr{C}_0$ as

$$\sum_{\varsigma_\kappa} [\widehat{\boldsymbol{\Sigma}}^* \cdot \widehat{\boldsymbol{N}}]^{\varsigma_\kappa} - [\widetilde{\operatorname{Div}} \widetilde{\boldsymbol{\Sigma}}^* + \widetilde{\boldsymbol{B}}_0]^\kappa =: \widetilde{\boldsymbol{B}}_0^{d\kappa} \quad \textit{on each } \mathscr{C}_0^\kappa \quad \textit{with } \widetilde{\boldsymbol{\Sigma}}^* := \widetilde{\boldsymbol{\Sigma}} + \widetilde{\boldsymbol{\Pi}}_0 \otimes \boldsymbol{T}. \tag{120}$$

The last statement is in turn supplemented by a Neumann-type boundary condition on the boundary points in $\mathscr{P}_0$ as

$$\sum_{\kappa_\pi} [\widetilde{\boldsymbol{\Sigma}}^* \cdot \widetilde{\boldsymbol{M}}]^{\kappa_\pi} - \bar{\boldsymbol{B}}^\pi =: \bar{\boldsymbol{B}}^{d\pi} \quad \textit{on each } \mathscr{P}_0^\pi. \tag{121}$$

Here the configurational stress in material description and the distributed force related to the bulk $\mathscr{B}_0$ follow as

$$\boldsymbol{\Sigma} := U_0 \boldsymbol{I} - \boldsymbol{F}^{\mathrm{t}} \cdot \partial_{\boldsymbol{F}} U_0 \quad \textit{and} \quad \boldsymbol{B}_0 := -\partial_{\boldsymbol{\Phi}} U_0. \tag{122}$$

Likewise, the configurational stress in material description and the distributed force related to the surfaces in $\mathscr{S}_0$ *are given by*

$$\widehat{\boldsymbol{\Sigma}} := u_0 \widehat{\boldsymbol{I}} - \widehat{\boldsymbol{F}}^{\mathrm{t}} \cdot \partial_{\widehat{\boldsymbol{F}}} u_0, \quad \widehat{\boldsymbol{B}}_0 := -\partial_{\boldsymbol{\Phi}} u_0. \tag{123}$$

Furthermore, the configurational stress in material description and the distributed force related to the curves in $\mathscr{C}_0$ *are given by*

$$\widetilde{\boldsymbol{\Sigma}} := \mathsf{u}_0 \widetilde{\boldsymbol{I}} - \widetilde{\boldsymbol{F}}^{\mathrm{t}} \cdot \partial_{\widetilde{\boldsymbol{F}}} \mathsf{u}_0, \quad \widetilde{\boldsymbol{B}}_0 := -\partial_{\boldsymbol{\Phi}} \mathsf{u}_0. \tag{124}$$

The configurational surface and curve shear $\widehat{\boldsymbol{\Pi}}_0$ *and* $\widetilde{\boldsymbol{\Pi}}_0$ *in material description related to* $\mathscr{S}_0$ *and* $\mathscr{C}_0$ *as well as the pointwise force* $\bar{\boldsymbol{B}}$ *related to* $\mathscr{P}_0$ *have been defined in* Eqs. (113)–(115).

Proof. Since $U_t = jU_0$, the material variation of the bulk potential energy density follows as

$$J\,\mathrm{d}_\delta[jU_0] = [U_0 \boldsymbol{I} - \boldsymbol{F}^{\mathrm{t}} \cdot \partial_{\boldsymbol{F}} U_0] : \mathrm{Grad}(\mathrm{d}_\delta \boldsymbol{\Phi}) + \partial_{\boldsymbol{\Phi}} \mathrm{U}_0 \cdot \mathrm{d}_\delta \boldsymbol{\Phi}.$$

Likewise, since $u_0 = \hat{j} u_0$, the material variation of the surface potential energy density follows with Eq. (47.2) as

$$\hat{J}\,\mathrm{d}_\delta[\hat{j}u_0] = [u_0 \widehat{\boldsymbol{I}} - \widehat{\boldsymbol{F}}^{\mathrm{t}} \cdot \partial_{\widehat{\boldsymbol{F}}} u_0 - \boldsymbol{N} \otimes \partial_{\boldsymbol{N}} u_0 \cdot \widehat{\boldsymbol{I}}] : \widehat{\mathrm{Grad}}(\mathrm{d}_\delta \boldsymbol{\Phi}) + \partial_{\boldsymbol{\Phi}} u_0 \cdot \mathrm{d}_\delta \boldsymbol{\Phi}.$$

Finally, since $\mathsf{u}_0 = \tilde{j} \mathsf{u}_0$, the material variation of the curve potential energy density follows with Eq. (64.2) as

$$\tilde{J}\,\mathrm{d}_\delta[\tilde{j}\mathsf{u}_0] = [\mathsf{u}_0 \widetilde{\boldsymbol{I}} - \widetilde{\boldsymbol{F}}^{\mathrm{t}} \cdot \partial_{\widetilde{\boldsymbol{F}}} \mathsf{u}_0 + \partial_{\boldsymbol{T}} \mathsf{u}_0 \cdot \widetilde{\boldsymbol{I}}^{\perp} \otimes \boldsymbol{T}] : \widetilde{\mathrm{Grad}}(\mathrm{d}_\delta \boldsymbol{\Phi}) + \partial_{\boldsymbol{\Phi}} \mathsf{u}_0 \cdot \mathrm{d}_\delta \boldsymbol{\Phi}.$$

Using further the definitions for the configurational stresses and distributed forces in Eqs. (122)–(124), (113)–(115), applying integration by parts and the divergence and especially the surface and curve divergence theorems in Eqs. (12), (26) while observing that $\widehat{\boldsymbol{\Sigma}}^* \cdot \boldsymbol{N} = \boldsymbol{0}$ and $\widetilde{\boldsymbol{\Sigma}}^* \cdot \boldsymbol{M} = 0$, renders

$$\begin{aligned}
\mathrm{d}_\delta I(\boldsymbol{\Phi}) = & -\int_{\mathscr{B}_0} [\,\mathrm{Div}\,\boldsymbol{\Sigma}^* + \boldsymbol{B}_0] \cdot \mathrm{d}_\delta \boldsymbol{\Phi}\,\mathrm{d}V \\
& - \sum_{\varsigma} \int_{\mathscr{S}_0^{\varsigma}} \left[\widehat{\mathrm{Div}}\,\widehat{\boldsymbol{\Sigma}}^* + \widehat{\boldsymbol{B}}_0 - \boldsymbol{\Sigma}^* \cdot \boldsymbol{N}\right] \cdot \mathrm{d}_\delta \boldsymbol{\Phi}\,\mathrm{d}A \\
& - \sum_{\kappa} \int_{\mathscr{C}_0^{\kappa}} \left[\widetilde{\mathrm{Div}}\,\widetilde{\boldsymbol{\Sigma}}^* + \widetilde{\boldsymbol{B}}_0 - \sum_{\varsigma_\kappa} \widehat{\boldsymbol{\Sigma}}^* \cdot \widehat{\boldsymbol{N}}\right] \cdot \mathrm{d}_\delta \boldsymbol{\Phi}\,\mathrm{d}L \\
& - \sum_{\pi} \left[\bar{\boldsymbol{B}} - \sum_{\kappa_\pi} \widetilde{\boldsymbol{\Sigma}}^* \cdot \widetilde{\boldsymbol{M}}\right] \cdot \mathrm{d}_\delta \boldsymbol{\Phi} =: \mathscr{R} \quad \forall\, \mathrm{d}_\delta \boldsymbol{\Phi}.
\end{aligned} \tag{125}$$

Finally, observing that the above statement has to be satisfied for all material variations of the material deformation map proves the theorem. □

Remark. Observe that the above derivation are valid if neither $\boldsymbol{\Sigma} \cdot \boldsymbol{N}$ nor $\widehat{\boldsymbol{\Sigma}}^* \cdot \widehat{\boldsymbol{N}}$ display a singularity when approaching a curve $\mathscr{C}_0^{\kappa}$ or a point $\mathscr{P}_0^{\pi}$, respectively. To consider singularities we have to account for the following additional contributions to Eqs. (108) and (109), respectively:

$$\widetilde{\boldsymbol{B}}_0^{s\kappa} := \lim_{r \to 0} \int_{\partial \mathscr{D}_0^{\kappa} \cap \mathscr{B}_0} \boldsymbol{\Sigma} \cdot \boldsymbol{N}\,\mathrm{d}\mathscr{L},$$

$$\bar{\boldsymbol{B}}^{s\pi} := \lim_{r \to 0} \int_{\partial \mathscr{B}_0^{\pi} \cap \mathscr{B}_0} \boldsymbol{\Sigma} \cdot \boldsymbol{N}\,\mathrm{d}\mathscr{A} + \sum_{\varsigma_\pi} \lim_{r \to 0} \int_{\partial \mathscr{B}_0^{\pi} \cap \mathscr{S}_0^{\varsigma_\pi}} \widehat{\boldsymbol{\Sigma}}^* \cdot \widehat{\boldsymbol{N}}\,\mathrm{d}\mathscr{L}.$$

Again, for the simplicity of exposition, we shall not explicitly indicate these contributions in the sequel, keeping in mind how and where to add terms if necessary.

Remark. The mixed-variant configurational two-point and material description stresses in the surfaces are related by surface pull-back/push-forward operations that are formally similar to the well-known pull-back/

push-forward operations of the stresses in the bulk

$$\widehat{\boldsymbol{p}} = \widehat{\boldsymbol{\Sigma}} \cdot \widehat{\operatorname{cof}} \widehat{\boldsymbol{f}} = \hat{j}\widehat{\Sigma}^{\beta}_{\alpha} \boldsymbol{A}^{\alpha} \otimes \boldsymbol{a}_{\beta}. \quad \text{and} \quad \widehat{\boldsymbol{\Sigma}} = \widehat{\boldsymbol{p}} \cdot \widehat{\operatorname{cof}} \widehat{\boldsymbol{F}} = \widehat{\Sigma}^{\beta}_{\alpha} \boldsymbol{A}^{\alpha} \otimes \boldsymbol{A}_{\beta}. \tag{126}$$

Thus, the configurational surface Eshelby-type stresses $\widehat{\boldsymbol{p}}$ and $\widehat{\boldsymbol{\Sigma}}$ are related by Piola transformations and, according to Eq. (54) and due to being tangential, satisfy $\widehat{\operatorname{div}} \widehat{\boldsymbol{p}} = \hat{j}\, \widehat{\operatorname{Div}}\, \widehat{\boldsymbol{\Sigma}}$. The corresponding surface pull-back/push-forward of the configurational surface shear, resulting in $\widehat{\operatorname{div}}\, \boldsymbol{s}_t = \hat{j}\, \widehat{\operatorname{Div}}\, \boldsymbol{\Pi}_0$, reads

$$\widehat{\boldsymbol{s}}_t = \widehat{\boldsymbol{\Pi}}_0 \cdot \widehat{\operatorname{cof}} \widehat{\boldsymbol{f}} = \widehat{\Pi}^{\beta}_{t} \boldsymbol{a}_{\beta} \quad \text{and} \quad \widehat{\boldsymbol{\Pi}}_0 = \widehat{\boldsymbol{s}}_t \cdot \widehat{\operatorname{cof}} \widehat{\boldsymbol{F}} = \widehat{\Pi}^{\beta}_{0} \boldsymbol{A}_{\beta}. \tag{127}$$

Likewise, the mixed-variant deformational two-point and material description stresses in the curves are related by curve pull-back/push-forward operations

$$\widetilde{\boldsymbol{p}} = \widetilde{\boldsymbol{\Sigma}} \cdot \widetilde{\operatorname{cof}} \widetilde{\boldsymbol{f}} = \widetilde{\Sigma}\, \boldsymbol{T} \otimes \boldsymbol{t} \quad \text{and} \quad \widetilde{\boldsymbol{\Sigma}} = \widetilde{\boldsymbol{p}} \cdot \widetilde{\operatorname{cof}} \widetilde{\boldsymbol{F}} = \widetilde{\Sigma}\, \boldsymbol{T} \otimes \boldsymbol{T}. \tag{128}$$

Thus, the configurational curve Eshelby-type stresses $\widetilde{\boldsymbol{p}}$ and $\widetilde{\boldsymbol{\Sigma}}$ are related by Piola transformations and, according to Eq. (70) and due to being tangential, satisfy $\widetilde{\operatorname{div}} \widetilde{\boldsymbol{p}} = \tilde{j}\, \widetilde{\operatorname{Div}}\, \widetilde{\boldsymbol{\sigma}}$.

Remark. Comparing the deformational surface stress in spatial description $\widehat{\boldsymbol{\sigma}}$ with the configurational surface stress in material description $\widehat{\boldsymbol{\Sigma}}$ reveals an intriguing formal similarity

$$\widehat{\boldsymbol{\sigma}} = u_t \widehat{\boldsymbol{i}} - \widehat{\boldsymbol{f}}^{\mathrm{t}} \cdot \widehat{\boldsymbol{p}}. \quad \text{and} \quad \widehat{\boldsymbol{\Sigma}} = u_0 \widehat{\boldsymbol{I}} - \widehat{\boldsymbol{F}}^{\mathrm{t}} \cdot \widehat{\boldsymbol{P}}. \tag{129}$$

Likewise, comparing the deformational curve stress in spatial description $\widetilde{\boldsymbol{\sigma}}$ with the configurational curve stress in material description $\widetilde{\boldsymbol{\Sigma}}$ renders

$$\widetilde{\boldsymbol{\sigma}} = \mathsf{u}_t \widetilde{\boldsymbol{i}} - \widetilde{\boldsymbol{f}}^{\mathrm{t}} \cdot \widetilde{\boldsymbol{p}}. \quad \text{and} \quad \widetilde{\boldsymbol{\Sigma}} = \mathsf{u}_0 \widetilde{\boldsymbol{I}} - \widetilde{\boldsymbol{F}}^{\mathrm{t}} \cdot \widetilde{\boldsymbol{P}}. \tag{130}$$

The formal similarities for the boundary stresses parallel known representations for the bulk stresses.

Remark. For regular solution fields in the bulk, i.e. fields that are as smooth as needed, it can easily be shown that the pull-back of the (localized) deformational force balance results in[5]

$$\boldsymbol{F}^{\mathrm{t}} \cdot [\operatorname{Div} \boldsymbol{P} + \boldsymbol{b}_0] = -[\operatorname{Div} \boldsymbol{\Sigma} + \boldsymbol{B}_0]. \tag{131}$$

As a consequence the configurational force $\boldsymbol{B}^d_0$, distributed in the bulk, vanishes in this case $\boldsymbol{B}^d_0 = \boldsymbol{0}$, i.e. the (localized) configurational force balance is trivially satisfied. The resulting relations between the four different versions of (localized) force balance in the bulk are depicted in Fig. 1.

Remark. For regular solution fields on a boundary surface ς, i.e. fields that are as smooth as needed, it can easily be shown that the surface pull-back of the (localized) deformational force balance on the surface results in[6]

$$-\widehat{\boldsymbol{F}}^{\mathrm{t}\varsigma} \cdot \left[\boldsymbol{P} \cdot \boldsymbol{N}^{\varsigma} - [\widehat{\operatorname{Div}}\, \widehat{\boldsymbol{P}}^{*} + \widehat{\boldsymbol{b}}_0]^{\varsigma}\right] = \widehat{\boldsymbol{I}}^{\varsigma} \cdot \left[\boldsymbol{\Sigma} \cdot \boldsymbol{N}^{\varsigma} - [\widehat{\operatorname{Div}} \widehat{\boldsymbol{\Sigma}}^{*} + \widehat{\boldsymbol{B}}_0]^{\varsigma}\right]. \tag{132}$$

As a consequence the tangential part of the configurational force $[\widehat{\boldsymbol{I}} \cdot \widehat{\boldsymbol{B}}^d_0]^{\varsigma}$, distributed in the boundary surface, vanishes in this case $[\widehat{\boldsymbol{I}} \cdot \widehat{\boldsymbol{B}}^d_0]^{\varsigma} = \boldsymbol{0}$, i.e. the tangential part of the (localized) configurational force balance on the

[5] Note the following intermediate results:

(i) $\operatorname{Div}(\boldsymbol{F}^{\mathrm{t}} \cdot \boldsymbol{P}) = \boldsymbol{F}^{\mathrm{t}} \cdot \operatorname{Div} \boldsymbol{P} + \boldsymbol{P} : \operatorname{Grad} \boldsymbol{F}$.
(ii) $\operatorname{Grad} U_0 = \operatorname{Div}(U_0 \boldsymbol{I}) = \boldsymbol{P} : \operatorname{Grad} \boldsymbol{F} - \boldsymbol{B}_0 - \boldsymbol{F}^{\mathrm{t}} \cdot \boldsymbol{b}_0$.

[6] Note the following intermediate results:

(i) $\widehat{\boldsymbol{I}} \cdot \boldsymbol{I} \cdot \boldsymbol{N} = \boldsymbol{0}$, $\widehat{\boldsymbol{I}} \cdot \boldsymbol{F}^{\mathrm{t}} = \widehat{\boldsymbol{F}}^{\mathrm{t}}$, thus $-\widehat{\boldsymbol{F}}^{\mathrm{t}} \cdot \boldsymbol{P} \cdot \boldsymbol{N} = \widehat{\boldsymbol{I}} \cdot \boldsymbol{\Sigma} \cdot \boldsymbol{N}$.
(ii) $\widehat{\operatorname{Div}}(\widehat{\boldsymbol{F}}^{\mathrm{t}} \cdot \widehat{\boldsymbol{P}}) = \widehat{\boldsymbol{F}}^{\mathrm{t}} \cdot \widehat{\operatorname{Div}} \widehat{\boldsymbol{P}} + \widehat{\boldsymbol{P}} : \widehat{\operatorname{Grad}} \widehat{\boldsymbol{F}} + [\widehat{\boldsymbol{F}}^{\mathrm{t}} \cdot \widehat{\boldsymbol{P}}] : \boldsymbol{K}\, \boldsymbol{N}$ due to Eq. (9).
(iii) $\widehat{\boldsymbol{F}}^{\mathrm{t}} \cdot \widehat{\operatorname{Div}}(\boldsymbol{n} \otimes \widehat{\boldsymbol{S}}_0) = -\widehat{\boldsymbol{F}}^{\mathrm{t}} \cdot \boldsymbol{k} \cdot \widehat{\boldsymbol{\pi}}_0$ and $\widehat{\boldsymbol{I}} \cdot \widehat{\operatorname{Div}}(\boldsymbol{N} \otimes \widehat{\boldsymbol{\Pi}}_0) = -\boldsymbol{K} \cdot \widehat{\boldsymbol{\Pi}}_0$.
(iv) $\widehat{\operatorname{Grad}}\, u_0 = \widehat{\operatorname{Div}}(u_0 \widehat{\boldsymbol{I}}) - u_0 K N = \widehat{\boldsymbol{P}} : \widehat{\operatorname{Grad}} \widehat{\boldsymbol{F}} - \widehat{\boldsymbol{I}} \cdot \widehat{\boldsymbol{B}}_0 - \widehat{\boldsymbol{F}}^{\mathrm{t}} \cdot \widehat{\boldsymbol{b}}_0 + \boldsymbol{K} \cdot \widehat{\boldsymbol{\Pi}}_0 + \widehat{\boldsymbol{F}}^{\mathrm{t}} \cdot \boldsymbol{k} \cdot \widehat{\boldsymbol{\pi}}_0$.

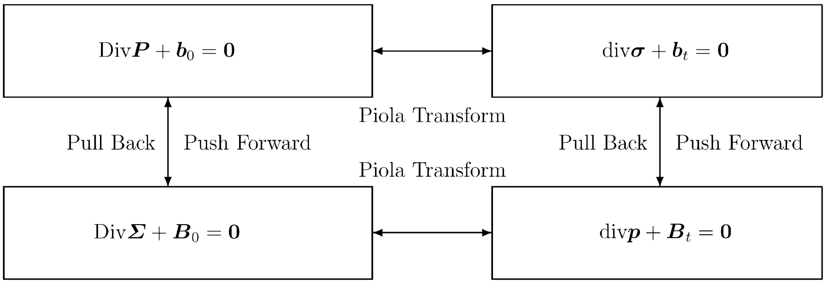

Fig. 1. (Localized) Force balance in the bulk.

boundary surface is trivially satisfied. The resulting relations between the four different versions of the tangential part of the (localized) force balance on the surface are depicted in Fig. 2.

Finally, the normal part of the configurational force $\widehat{\boldsymbol{B}}_0^{d\varsigma}$ on the boundary surface ς, i.e.

$$[\boldsymbol{N} \cdot \widehat{\boldsymbol{B}}_0^d]^\varsigma = \boldsymbol{N}^\varsigma \cdot [\boldsymbol{\Sigma} \cdot \boldsymbol{N}^\varsigma - [\widehat{\mathrm{Div}}\, \widehat{\boldsymbol{\Sigma}}^* + \widehat{\boldsymbol{B}}_0]^\varsigma] =: \widehat{B}_0^{d\varsigma}$$

distributed in a boundary surface and responsible for energetic changes that go along with configurational changes follows as

$$\boldsymbol{N}^\varsigma \cdot \boldsymbol{\Sigma} \cdot \boldsymbol{N}^\varsigma - [\widehat{\boldsymbol{\Sigma}} : \boldsymbol{K} + \widehat{\mathrm{Div}} \widehat{\boldsymbol{\Pi}}_0 + \boldsymbol{N} \cdot \widehat{\boldsymbol{B}}_0]^\varsigma =: \widehat{B}_0^{d\varsigma}. \tag{133}$$

The first term in Eq. (133) is the contribution from the bulk in terms of the configurational (Eshelby) stress in Eq. (122), which can be rewritten due to the (localized) deformational force balance for the surfaces in Eq. (77) as

$$\boldsymbol{N}^\varsigma \cdot \boldsymbol{\Sigma} \cdot \boldsymbol{N}^\varsigma = U_0 - \boldsymbol{N}^\varsigma \cdot \boldsymbol{F}^{\mathrm{t}} \cdot [\widehat{\mathrm{Div}}\, \widehat{\boldsymbol{P}}^* + \widehat{\boldsymbol{b}}_0]^\varsigma. \tag{134}$$

The remaining terms in Eq. (133) relate to the configurational surface stress, the curvature of the boundary surface and the configurational surface shear and distributed force. An equivalent result for the case of interfaces has earlier been obtained e.g. by Leo and Sekerka (1989), Gurtin and Struthers (1990), Gurtin (1995), cf. also references therein.

Remark. For regular solution fields on a boundary curve κ, i.e. fields that are as smooth as needed, it can easily be shown that the curve pull-back of the (localized) deformational force balance on the curve results in[7]

$$-\widetilde{\boldsymbol{F}}^{\mathrm{t}\kappa} \cdot \left[\sum_{\varsigma_\kappa} [\widehat{\boldsymbol{P}}^* \cdot \widehat{\boldsymbol{N}}]^{\varsigma_\kappa} - [\widetilde{\mathrm{Div}} \widetilde{\boldsymbol{P}}^* + \widetilde{\boldsymbol{b}}_0]^\kappa \right] = \widetilde{\boldsymbol{I}}^\kappa \cdot \left[\sum_{\varsigma_\kappa} [\widehat{\boldsymbol{\Sigma}}^* \cdot \widehat{\boldsymbol{N}}]^{\varsigma_\kappa} - [\widetilde{\mathrm{Div}} \widetilde{\boldsymbol{\Sigma}}^* + \widetilde{\boldsymbol{B}}_0]^\kappa \right]. \tag{135}$$

As a consequence the tangential part of the configurational force $[\widetilde{\boldsymbol{I}} \cdot \widetilde{\boldsymbol{B}}_0^d]^\kappa$, distributed in the boundary curve, vanishes in this case $[\widetilde{\boldsymbol{I}} \cdot \widetilde{\boldsymbol{B}}_0^d]^\kappa = \mathbf{0}$, i.e. the tangential part of the (localized) configurational force balance on the boundary curve is trivially satisfied. The resulting relations between the four different versions of the tangential part of the (localized) force balance on the curve are depicted in Fig. 3.

Finally, the part of the configurational force $\widetilde{\boldsymbol{B}}_0^{d\kappa}$ perpendicular to the tangent of curve κ, i.e.

$$[\widetilde{\boldsymbol{I}}^\perp \cdot \widetilde{\boldsymbol{B}}_0^d]^\kappa = \widetilde{\boldsymbol{I}}^{\perp\kappa} \cdot \left[\sum_{\varsigma_\kappa} [\widehat{\boldsymbol{\Sigma}}^* \cdot \widehat{\boldsymbol{N}}]^{\varsigma_\kappa} - [\widetilde{\mathrm{Div}}\, \widetilde{\boldsymbol{\Sigma}}^* + \widetilde{\boldsymbol{B}}_0]^\kappa \right] =: \widetilde{\boldsymbol{B}}_0^{d\perp\kappa}$$

[7]Note the following intermediate results:

(i) $\widetilde{\boldsymbol{I}} \cdot \widehat{\boldsymbol{I}} = \widetilde{\boldsymbol{I}}$ renders $\widetilde{\boldsymbol{I}} \cdot \widehat{\boldsymbol{I}} \cdot \widehat{\boldsymbol{N}} = \mathbf{0}$, $\widetilde{\boldsymbol{I}} \cdot \widehat{\boldsymbol{F}}^{\mathrm{t}} = \widetilde{\boldsymbol{F}}^{\mathrm{t}}$, moreover $\widetilde{\boldsymbol{F}}^{\mathrm{t}} \cdot \boldsymbol{n} = \mathbf{0}$ and $\widetilde{\boldsymbol{I}} \cdot \boldsymbol{N} = \mathbf{0}$, thus $-\widetilde{\boldsymbol{F}}^{\mathrm{t}} \cdot \widehat{\boldsymbol{P}}^* \cdot \widehat{\boldsymbol{N}} = \widetilde{\boldsymbol{I}} \cdot \widehat{\boldsymbol{\Sigma}}^* \cdot \widehat{\boldsymbol{N}}$.
(ii) $\widetilde{\mathrm{Div}}(\widetilde{\boldsymbol{F}}^{\mathrm{t}} \cdot \widetilde{\boldsymbol{P}}) = \widetilde{\boldsymbol{F}}^{\mathrm{t}} \cdot \widetilde{\mathrm{Div}} \widetilde{\boldsymbol{P}} + \widetilde{\boldsymbol{P}} : \widetilde{\mathrm{Grad}}\, \widetilde{\boldsymbol{F}} + [\widetilde{\boldsymbol{F}}^{\mathrm{t}} \cdot \widetilde{\boldsymbol{P}}] : \boldsymbol{C}_\perp \boldsymbol{M}$ due to Eq. (23).
(iii) $\widetilde{\boldsymbol{F}}^{\mathrm{t}} \cdot \widetilde{\mathrm{Div}}(\widetilde{\boldsymbol{\pi}}_t \otimes \boldsymbol{T}) = -\widetilde{\boldsymbol{F}}^{\mathrm{t}} \cdot \boldsymbol{c}_\parallel^{\mathrm{t}} \cdot \widetilde{\boldsymbol{\pi}}_0$ and $\widetilde{\boldsymbol{I}} \cdot \widetilde{\mathrm{Div}}(\widetilde{\boldsymbol{\Pi}}_0 \otimes \boldsymbol{T}) = -\boldsymbol{C}_\parallel^{\mathrm{t}} \cdot \widetilde{\boldsymbol{\Pi}}_0$.
(iv) $\widetilde{\mathrm{Grad}}\, \mathsf{u}_0 = \widetilde{\mathrm{Div}}(\mathsf{u}_0 \widetilde{\boldsymbol{I}}) - \mathsf{u}_0 \mathsf{C} \boldsymbol{M} = \widetilde{\boldsymbol{P}} : \widetilde{\mathrm{Grad}}\, \widetilde{\boldsymbol{F}} - \widetilde{\boldsymbol{I}} \cdot \widetilde{\boldsymbol{B}}_0 - \widetilde{\boldsymbol{F}}^{\mathrm{t}} \cdot \widetilde{\boldsymbol{b}}_0 + \boldsymbol{C}_\parallel^{\mathrm{t}} \cdot \widetilde{\boldsymbol{\Pi}}_0 + \widetilde{\boldsymbol{F}}^{\mathrm{t}} \cdot \boldsymbol{c}_\parallel^{\mathrm{t}} \cdot \widetilde{\boldsymbol{\pi}}_0$.

(*) For the case of singularities $-\widetilde{\boldsymbol{F}}^{\mathrm{t}} \cdot \widetilde{\boldsymbol{b}}_0^s = \widetilde{\boldsymbol{I}} \cdot \widetilde{\boldsymbol{B}}_0^s$ can be shown along the same lines.

$$
\begin{tikzcd}
\widehat{\boldsymbol{i}}^{\varsigma}\cdot\left[\boldsymbol{P}\cdot\boldsymbol{N}^{\varsigma}-[\widehat{\mathrm{Div}}\widehat{\boldsymbol{P}}^{*}+\widehat{\boldsymbol{b}}_{0}]^{\varsigma}\right]=\boldsymbol{0} \arrow[r, leftrightarrow, "\text{Surface Piola Transform}"'] \arrow[d, leftrightarrow, "\text{Surface Pull Back}"', "\text{Surface Push Forward}"] & \widehat{\boldsymbol{i}}^{\varsigma}\cdot\left[\boldsymbol{\sigma}\cdot\boldsymbol{n}^{\varsigma}-[\widehat{\mathrm{div}}\widehat{\boldsymbol{\sigma}}^{*}+\widehat{\boldsymbol{b}}_{t}]^{\varsigma}\right]=\boldsymbol{0} \arrow[d, leftrightarrow, "\text{Surface Pull Back}"', "\text{Surface Push Forward}"] \\
\widehat{\boldsymbol{I}}^{\varsigma}\cdot\left[\boldsymbol{\Sigma}\cdot\boldsymbol{N}^{\varsigma}-[\widehat{\mathrm{Div}}\widehat{\boldsymbol{\Sigma}}^{*}+\widehat{\boldsymbol{B}}_{0}]^{\varsigma}\right]=\boldsymbol{0} \arrow[r, leftrightarrow, "\text{Surface Piola Transform}"] & \widehat{\boldsymbol{I}}^{\varsigma}\cdot\left[\boldsymbol{p}\cdot\boldsymbol{n}^{\varsigma}-[\widehat{\mathrm{div}}\widehat{\boldsymbol{p}}^{*}+\widehat{\boldsymbol{B}}_{t}]^{\varsigma}\right]=\boldsymbol{0}
\end{tikzcd}
$$

Fig. 2. Tangential part of the (localized) force balance on the surface ς.

$$
\begin{tikzcd}
\widetilde{\boldsymbol{i}}^{\kappa}\cdot\left[\sum_{\varsigma_\kappa}[\widehat{\boldsymbol{P}}^{*}\cdot\widehat{\boldsymbol{N}}]^{\varsigma_\kappa}-[\widetilde{\mathrm{Div}}\widetilde{\boldsymbol{P}}^{*}+\widetilde{\boldsymbol{b}}_{0}]^{\kappa}\right]=\boldsymbol{0} \arrow[r, leftrightarrow, "\text{Curve Piola Transform}"'] \arrow[d, leftrightarrow, "\text{Curve Pull Back}"', "\text{Curve Push Forward}"] & \widetilde{\boldsymbol{i}}^{\kappa}\cdot\left[\sum_{\varsigma_\kappa}[\widehat{\boldsymbol{\sigma}}^{*}\cdot\widehat{\boldsymbol{n}}]^{\varsigma_\kappa}-[\widetilde{\mathrm{div}}\widetilde{\boldsymbol{\sigma}}^{*}+\widetilde{\boldsymbol{b}}_{0}]^{\kappa}\right]=\boldsymbol{0} \arrow[d, leftrightarrow, "\text{Curve Pull Back}"', "\text{Curve Push Forward}"] \\
\widetilde{\boldsymbol{I}}^{\kappa}\cdot\left[\sum_{\varsigma_\kappa}[\widehat{\boldsymbol{\Sigma}}^{*}\cdot\widehat{\boldsymbol{N}}]^{\varsigma_\kappa}-[\widetilde{\mathrm{Div}}\widetilde{\boldsymbol{\Sigma}}^{*}+\widetilde{\boldsymbol{B}}_{0}]^{\kappa}\right]=\boldsymbol{0} \arrow[r, leftrightarrow, "\text{Curve Piola Transform}"] & \widetilde{\boldsymbol{I}}^{\kappa}\cdot\left[\sum_{\varsigma_\kappa}[\widehat{\boldsymbol{p}}^{*}\cdot\widehat{\boldsymbol{n}}]^{\varsigma_\kappa}-[\widetilde{\mathrm{div}}\widetilde{\boldsymbol{p}}^{*}+\widetilde{\boldsymbol{B}}_{0}]^{\kappa}\right]=\boldsymbol{0}
\end{tikzcd}
$$

Fig. 3. Tangential part of the (localized) force balance on the curve κ.

distributed along the boundary curve and responsible for energetic changes that go along with configurational changes, follows as

$$\sum_{\varsigma_\kappa}[[\widehat{\boldsymbol{N}}\cdot\widehat{\boldsymbol{\Sigma}}\cdot\widehat{\boldsymbol{N}}]\,\widehat{\boldsymbol{N}}+[\widehat{\boldsymbol{\Pi}}_0\cdot\widehat{\boldsymbol{N}}]\,\boldsymbol{N}]^{\varsigma_\kappa}-[[\widetilde{\boldsymbol{\Sigma}}:\boldsymbol{C}_\perp]\boldsymbol{M}+\widetilde{\boldsymbol{I}}^{\perp}\cdot[\partial_\Theta\widetilde{\boldsymbol{\Pi}}_0+\widetilde{\boldsymbol{B}}_0]]^{\kappa}=:\widetilde{\boldsymbol{B}}_0^{d\perp\kappa}. \tag{136}$$

The sum is the contribution from the intersecting boundary surfaces in terms of the configurational surface (Eshelby) stress and shear in Eqs. (123), (114). The remaining terms in Eq. (136) relate to the configurational curve stress, the curvature of the boundary curve and the configurational curve shear and distributed force. A similar result for the case of interfaces has been obtained by Simha and Bhattacharya (2000).

Remark. Considering the decomposition of the surface potential energy density u_0 into the internal and external surface potential energy density w_0 and v_0 with $v_0=v_0(\boldsymbol{\Phi},\boldsymbol{N};\boldsymbol{\varphi},\boldsymbol{n})$ allows an alternative expression for the following contribution to the tangential part of the (localized) configurational force balance at surfaces

$$\widehat{\boldsymbol{I}}\cdot[\,\widehat{\mathrm{Div}}\,\widehat{\boldsymbol{\Sigma}}+\widehat{\boldsymbol{B}}_0-\boldsymbol{K}\cdot\widehat{\boldsymbol{\Pi}}_0]=\widehat{\boldsymbol{I}}\cdot[\,\widehat{\mathrm{Div}}\,\widehat{\boldsymbol{\Sigma}}^{i}+[\widehat{\boldsymbol{B}}_0^{i}-\widehat{\boldsymbol{F}}^{\mathrm{t}}\cdot\widehat{\boldsymbol{b}}_0]-[\boldsymbol{K}\cdot\widehat{\boldsymbol{\Pi}}_0^{i}-\widehat{\boldsymbol{F}}^{\mathrm{t}}\cdot\boldsymbol{k}\cdot\widehat{\boldsymbol{\pi}}_0]]. \tag{137}$$

Here, for the representation on the left hand side the result $\widehat{\mathrm{Div}}(\boldsymbol{N}\otimes\widehat{\boldsymbol{\Pi}}_0)=\boldsymbol{N}\,\widehat{\mathrm{Div}}\,\widehat{\boldsymbol{\Pi}}_0-\boldsymbol{K}\cdot\widehat{\boldsymbol{\Pi}}_0$ has been incorporated. On the right hand side $\widehat{\boldsymbol{\Sigma}}^{i}$, $\widehat{\boldsymbol{B}}_0^{i}$ and $\widehat{\boldsymbol{\Pi}}_0^{i}$ are defined as in Eqs. (123.1), (123.2) and (114) with the total surface potential energy density u_0 substituted by the internal surface potential energy density w_0. Then the result in Eq. (137) is obtained by computing the surface gradient of the external surface potential energy density v_0

$$\widehat{\mathrm{Grad}}\,v_0=-\widehat{\boldsymbol{I}}\cdot\widehat{\boldsymbol{B}}_0^{e}+\boldsymbol{K}\cdot\widehat{\boldsymbol{\Pi}}_0^{e}-\widehat{\boldsymbol{F}}^{\mathrm{t}}\cdot\widehat{\boldsymbol{b}}_0+\widehat{\boldsymbol{F}}^{\mathrm{t}}\cdot\boldsymbol{k}\cdot\widehat{\boldsymbol{\pi}}_0=\widehat{\mathrm{Div}}(v_0\widehat{\boldsymbol{I}})-v_0K\boldsymbol{N}. \tag{138}$$

Here, $\widehat{\boldsymbol{B}}_0^{e}$ and $\widehat{\boldsymbol{\Pi}}_0^{e}$ are defined as in Eqs. (123.2) and (114)) with the total surface potential energy density u_0 substituted by the external surface potential energy density v_0. Considering the tangential parts of Eq. (138) finally proves the result in Eq. (137). Arguing along the same lines renders also an alternative expression for the following contribution to the tangential part of the (localized) configurational force balance at curves with obvious notation

$$\widetilde{\boldsymbol{I}}\cdot[\,\widetilde{\operatorname{Div}}\,\widehat{\boldsymbol{\Sigma}}+\widetilde{\boldsymbol{B}}_0-\boldsymbol{C}_{\|}^{t}\cdot\widetilde{\boldsymbol{\Pi}}_0]=\widetilde{\boldsymbol{I}}\cdot[\,\widetilde{\operatorname{Div}}\,\widetilde{\boldsymbol{\Sigma}}^{i}+[\widetilde{\boldsymbol{B}}_0^{i}-\widetilde{\boldsymbol{F}}^{\mathrm{t}}\cdot\widetilde{\boldsymbol{b}}_0]-[\boldsymbol{C}_{\|}^{t}\cdot\widetilde{\boldsymbol{\Pi}}_0^{i}-\widetilde{\boldsymbol{F}}^{\mathrm{t}}\cdot\boldsymbol{c}_{\|}^{t}\cdot\widetilde{\boldsymbol{\pi}}_0]]. \tag{139}$$

The results in Eqs. (137), (139) resemble known relations for the (localized) configurational force balance in the bulk, see e.g. Steinmann (2002a).

6. Some illustrating examples

In this section the general results obtained in the above shall be illuminated by some elementary examples of specific boundary potentials. In this way, individual terms in the resulting balance equations can be attributed to the increasing complexity in the format of the boundary potentials.

6.1. *Zero boundary potentials* $\{u_0, \mathsf{u}_0, \mathrm{u}\} = 0$

For the case of zero boundary potentials $\{u_0, \mathsf{u}_0, \mathrm{u}\} = 0$ the (localized) deformational and configurational force balances in Eqs. (77) and (119) are non-trivial and take the format

$$\boldsymbol{P}\cdot\boldsymbol{N}^{\varsigma}=\mathbf{0} \quad \text{and} \quad U_0=:\widehat{B}_0^{d\varsigma}. \tag{140}$$

Thus, in order to release potential energy, see Eqs. (104) and (105), an admissible material variation $\mathrm{d}_\delta\boldsymbol{\Phi}$ at $\mathscr{S}_0^{\varsigma}$ has to oppose the outward normal direction $\boldsymbol{N}^{\varsigma}$.

6.2. *Configurational boundary tension* $\{u_0, \mathsf{u}_0, \mathrm{u}\}$ =*constant*

For the case of configurational boundary tension with $\{u_0, \mathsf{u}_0, \mathrm{u}\}$ =constant the (localized) deformational and configurational force balances in Eqs. (77) and (119) are non-trivial and take the format

$$\boldsymbol{P}\cdot\boldsymbol{N}^{\varsigma}=\mathbf{0} \quad \text{and} \quad U_0-[u_0\,K]^{\varsigma}=:\widehat{B}_0^{d\varsigma}. \tag{141}$$

This result applies e.g. to boundary tension in crystalline materials, see e.g. Gurtin (2000). It appears that potential energy release due to the bulk potential energy is competing with the effects of configurational surface tension and curvature. Thus for a sufficiently large positive curvature $K>0$ so that $U_0-u_0\,K<0$ an admissible material variation $\mathrm{d}_\delta\boldsymbol{\Phi}$ at $\mathscr{S}_0$ even has to point towards the outward normal direction $\boldsymbol{N}^{\varsigma}$ in order to release potential energy in correspondence with Eqs. (104) and (105). A positive curvature corresponds to a locally concave body as for example in the case of a cracked body with a rounded crack tip. In general, due to the contribution $-u_0\,K$ configurational surface tension may act as an obstacle to further crack extension.

For completeness, the remaining non-trivial (localized) configurational force balances in Eqs. (120) and (121) read

$$\sum_{\varsigma_\kappa}[u_0\,\widehat{\boldsymbol{N}}]^{\varsigma_\kappa}-[\mathsf{u}_0\,\mathsf{C}\,\boldsymbol{M}]^{\kappa}=:\widetilde{\boldsymbol{B}}_0^{d\perp\kappa} \quad \text{and} \quad \sum_{\kappa_\pi}[\mathsf{u}_0\,\widetilde{\boldsymbol{M}}]^{\kappa_\pi}=:\bar{\boldsymbol{B}}^{d\pi}. \tag{142}$$

6.3. *Deformational boundary tension* $\{u_t, \mathsf{u}_t, \mathrm{u}\}$ = constant

For the case of deformational boundary tension with $\{u_t, \mathsf{u}_t, \mathrm{u}\}$ = constant the (localized) deformational and configurational force balances in Eqs. (89) and (107) are non-trivial and take the format

$$\boldsymbol{\sigma}\cdot\boldsymbol{n}^{\varsigma}-[u_t\,k\,\boldsymbol{n}]^{\varsigma}=\mathbf{0} \quad \text{and} \quad U_0-J[u_t\,k]^{\varsigma}=\widehat{B}_0^{d\varsigma}. \tag{143}$$

The relation $\boldsymbol{\sigma}\cdot\boldsymbol{n}^{\varsigma}=[u_t\,k\,\boldsymbol{n}]^{\varsigma}$ corresponds to the celebrated Laplace–Young relation that applies e.g. to uncontaminated interfaces between immiscible fluids.

The remaining non-trivial (localized) deformational force balances in Eqs. (90) and (91) can be considered as Laplace–Young relations generalised to curves and points. They read

$$\sum_{\varsigma_\kappa}[u_t\,\widehat{\boldsymbol{n}}]^{\varsigma_\kappa} - [\mathsf{u}_t\,\mathsf{c}\,\boldsymbol{m}]^{\kappa} = \boldsymbol{0} \quad \text{and} \quad \sum_{\kappa_\pi}[\mathsf{u}_t\,\widetilde{\boldsymbol{m}}]^{\kappa_\pi} = \boldsymbol{0}. \tag{144}$$

In the above results we essentially used (93), (94) for the deformational surface and curve stresses in spatial description $\widehat{\boldsymbol{\sigma}} = u_t\widehat{\boldsymbol{i}}$ and $\widetilde{\boldsymbol{\sigma}} = \mathsf{u}_t\widetilde{\boldsymbol{i}}$ together with $\widehat{\operatorname{div}}\,\widehat{\boldsymbol{i}} = k\,\boldsymbol{n}$ and $\widetilde{\operatorname{div}}\,\widetilde{\boldsymbol{i}} = \mathsf{c}\,\boldsymbol{m}$ (see Eqs. (11), (24)).

6.4. Isotropic boundary traction $\{u_0, \mathsf{u}_0, \mathrm{u}\} = \{u_0, \mathsf{u}_0, \mathrm{u}\}(\boldsymbol{\varphi}; \boldsymbol{X})$

For the common case of isotropic boundary traction with $\{u_0, \mathsf{u}_0, \mathrm{u}\} = \{u_0, \mathsf{u}_0, \mathrm{u}\}(\boldsymbol{\varphi}; \boldsymbol{X})$ the (localized) deformational and configurational force balances in Eqs. (77) and (119) are non-trivial and take the format

$$\boldsymbol{P}\cdot\boldsymbol{N}^{\varsigma} + \partial_{\boldsymbol{\varphi}} u_0^{\varsigma} = \boldsymbol{0} \quad \text{and} \quad U_0 + [\nabla_N u_0 - u_0\,K]^{\varsigma} =: \widehat{B}_0^{d\varsigma}. \tag{145}$$

Again it appears that there is a competition between potential energy release due to the bulk potential energy and the (total) gradient of the surface potential energy in normal direction $\nabla_N u_0 := \nabla_{\boldsymbol{\Phi}} u_0 \cdot \boldsymbol{N}$ (with $\nabla_{\boldsymbol{\Phi}} u_0 := \partial_{\boldsymbol{\varphi}} u_0 \cdot \boldsymbol{F} + \partial_{\boldsymbol{\Phi}} u_0$) with the effects of surface tension and curvature.

The remaining non-trivial (localized) deformational force balances in Eqs. (78) and (79) read

$$\partial_{\boldsymbol{\varphi}} \mathsf{u}_0^{\kappa} = \widetilde{\boldsymbol{b}}_0^{s\kappa} \quad \text{and} \quad \partial_{\boldsymbol{\varphi}} \mathrm{u}^{\pi} = \bar{\boldsymbol{b}}^{s\pi}. \tag{146}$$

Here, the contributions $\widetilde{\boldsymbol{b}}_0^{s\kappa}$ and $\bar{\boldsymbol{b}}^{s\pi}$ due to the stress singularities introduced by the line and point loads (compare e.g. to the so-called Flament problem of a single force on a half space) have been considered.

Likewise, the remaining non-trivial (localized) configurational force balances in Eqs. (120), (121) read

$$\sum_{\varsigma_\kappa}[u_0\widehat{\boldsymbol{N}}]^{\varsigma_\kappa} + [\partial^{\perp}_{\boldsymbol{\Phi}}\mathsf{u}_0 - \mathsf{u}_0\,\mathsf{C}\,\boldsymbol{M}]^{\kappa} =: [\widetilde{\boldsymbol{B}}_0^{d} + \widetilde{\boldsymbol{B}}_0^{s}]^{\perp\kappa}, \tag{147}$$

$$\sum_{\kappa_\pi}[\mathsf{u}_0\widetilde{\boldsymbol{M}}]^{\kappa_\pi} + \partial_{\boldsymbol{\Phi}}\mathrm{u}^{\pi} =: [\bar{\boldsymbol{B}}^{d} + \bar{\boldsymbol{B}}^{s}]^{\pi}.$$

Again, the contributions $\widetilde{\boldsymbol{B}}_0^{s\kappa}$ and $\bar{\boldsymbol{B}}^{s\pi}$ are introduced in order to capture the stress singularities due to the line and point loads.

6.5. Isotropic boundary stress $\{u_0, \mathsf{u}_0, \mathrm{u}\} = \{u_0, \mathsf{u}_0, \mathrm{u}\}(\boldsymbol{\varphi}, \{\hat{\mathbf{F}}, \tilde{\mathbf{F}}, \emptyset\}; \boldsymbol{X})$

For the case of isotropic boundary stress with $\{u_0, \mathsf{u}_0, \mathrm{u}\} = \{u_0, \mathsf{u}_0, \mathrm{u}\}(\boldsymbol{\varphi}, \{\widehat{\boldsymbol{F}}, \widetilde{\boldsymbol{F}}, \emptyset\}; \boldsymbol{X})$ the (localized) deformational and configurational force balances in Eqs. (77) and (119) are non-trivial and take the format

$$\boldsymbol{P}\cdot\boldsymbol{N}^{\varsigma} + \widehat{\delta}_{\boldsymbol{\varphi}} u_0^{\varsigma} = \boldsymbol{0} \quad \text{and} \quad U_0 + [\widehat{\Delta}_N u_0 - u_0\,K + [\widehat{\boldsymbol{F}}^{\mathrm{t}}\cdot\partial_{\widehat{\boldsymbol{F}}} u_0] : \boldsymbol{K}]^{\varsigma} =: \widehat{B}_0^{d\varsigma}. \tag{148}$$

Here $\widehat{\delta}_{\boldsymbol{\varphi}} u_0 := \partial_{\boldsymbol{\varphi}} u_0 - \widehat{\operatorname{Div}}\,\partial_{\widehat{\boldsymbol{F}}} u_0$ abbreviates the variational surface derivative. Again it appears that there is a competition between potential energy release due to the bulk potential energy and the total variational surface derivative of the surface potential energy in normal direction $\widehat{\Delta}_N u_0 := \widehat{\Delta}_{\boldsymbol{\Phi}} u_0 \cdot \boldsymbol{N}$ (with $\widehat{\Delta}_{\boldsymbol{\Phi}} u_0 := \widehat{\delta}_{\boldsymbol{\varphi}} u_0 \cdot \boldsymbol{F} + \partial_{\boldsymbol{\Phi}} u_0$) with the effects of surface tension and curvature.

The remaining non-trivial (localized) deformational force balances in Eqs. (78) and (79) read

$$\sum_{\varsigma_\kappa}[\partial_{\widehat{\boldsymbol{F}}} u_0 \cdot \widehat{\boldsymbol{N}}]^{\varsigma_\kappa} + \widetilde{\delta}_{\boldsymbol{\varphi}} \mathsf{u}_0^{\kappa} = \boldsymbol{0} \quad \text{and} \quad \sum_{\kappa_\pi}[\partial_{\widetilde{\boldsymbol{F}}} \mathsf{u}_0 \cdot \widetilde{\boldsymbol{M}}]^{\kappa_\pi} + \partial_{\boldsymbol{\varphi}} \mathrm{u}^{\pi} = \boldsymbol{0}. \tag{149}$$

Here $\widetilde{\delta}_{\boldsymbol{\varphi}} \mathsf{u}_0 := \partial_{\boldsymbol{\varphi}} \mathsf{u}_0 - \widetilde{\operatorname{Div}}\,\partial_{\widetilde{\boldsymbol{F}}} \mathsf{u}_0$ abbreviates the variational curve derivative.

Likewise, the remaining non-trivial (localized) configurational force balances in Eqs. (120) and (121) read

$$\sum_{\varsigma_\kappa}[u_0\widehat{\boldsymbol{N}} + \widehat{\boldsymbol{F}}^{\perp t} \cdot \partial_{\widetilde{\boldsymbol{F}}} u_0 \cdot \widehat{\boldsymbol{N}}]^{\varsigma_\kappa} + [\widetilde{\Delta}^{\perp}_{\boldsymbol{\Phi}} \mathsf{u}_0 - \mathsf{u}_0\, \mathsf{C}\, \boldsymbol{M} + [\widetilde{\boldsymbol{F}}^{t} \cdot \partial_{\widetilde{\boldsymbol{F}}} \mathsf{u}_0] : \boldsymbol{C}_{\perp}]^{\kappa} := \widetilde{\boldsymbol{B}}^{d\perp\kappa}_0$$

$$\sum_{\kappa_\pi}[\mathsf{u}_0\widetilde{\boldsymbol{M}} + \widetilde{\boldsymbol{F}}^{\perp t} \cdot \partial_{\widetilde{\boldsymbol{F}}} \mathsf{u}_0 \cdot \widetilde{\boldsymbol{M}}]^{\kappa_\pi} + \nabla_{\boldsymbol{\Phi}} \mathsf{u}^{\pi} =: \bar{\boldsymbol{B}}^{d\pi}. \tag{150}$$

Here $\widetilde{\Delta}^{\perp}_{\boldsymbol{\Phi}}\mathsf{u}_0 := \widetilde{\Delta}_{\boldsymbol{\Phi}}\mathsf{u}_0 \cdot \widetilde{\boldsymbol{I}}^{\perp}$ with $\widetilde{\Delta}_{\boldsymbol{\Phi}}\mathsf{u}_0 := \widetilde{\delta}_{\boldsymbol{\varphi}}\mathsf{u}_0 \cdot \boldsymbol{F} + \partial_{\boldsymbol{\Phi}}\mathsf{u}_0$ abbreviates the total variational curve derivative in the direction perpendicular to $\boldsymbol{T}$. Moreover, we defined $\widehat{\boldsymbol{F}}^{\perp} := \boldsymbol{F} - \widehat{\boldsymbol{F}} = \boldsymbol{F} \cdot [\boldsymbol{N} \otimes \boldsymbol{N}]$ and $\widetilde{\boldsymbol{F}}^{\perp} := \boldsymbol{F} - \widetilde{\boldsymbol{F}} = \boldsymbol{F} \cdot [\boldsymbol{I} - \boldsymbol{T} \otimes \boldsymbol{T}]$.

6.6. Anisotropic boundary potential energy density

In order to account for anisotropies in the boundary potential energies a proposal by Gasser and Holzapfel (2003) (within the modelling of cohesive zones between soft biological tissues) may be adopted. Thus, e.g. the anisotropic part of the surface potential energy density may be represented in terms of the following invariants:

$$\widehat{I}_k = [\boldsymbol{\varphi} \otimes \boldsymbol{\varphi}]^k : [\boldsymbol{n} \otimes \boldsymbol{n}] \quad \text{and} \quad \widehat{i}_k = [\boldsymbol{\Phi} \otimes \boldsymbol{\Phi}]^k : [\boldsymbol{N} \otimes \boldsymbol{N}]. \tag{151}$$

The corresponding derivatives of the $\widehat{I}_k$ and $\widehat{i}_k$ with respect to the surface normals $\boldsymbol{n}$ and $\boldsymbol{N}$ then render the essential contributions to the deformational and configurational surface shear $\widehat{\boldsymbol{\pi}}_t$ and $\widehat{\boldsymbol{\pi}}_0$, respectively,

$$\partial_{\boldsymbol{n}}\widehat{I}_k = 2[\boldsymbol{\varphi} \otimes \boldsymbol{\varphi}]^k \cdot \boldsymbol{n} \quad \text{and} \quad \partial_{\boldsymbol{N}}\widehat{i}_k = 2[\boldsymbol{\Phi} \otimes \boldsymbol{\Phi}]^k \cdot \boldsymbol{N}. \tag{152}$$

Observe that the derivatives in Eq. (152) render a vector coaxial to $\boldsymbol{\varphi}$ and $\boldsymbol{\Phi}$, respectively, that are mapped by $\widehat{\boldsymbol{i}}$ and $\widehat{\boldsymbol{I}}$ for the computation of the deformational and configurational surface shear in Eqs. (84) and (114), respectively. Equivalent invariants can be constructed for the anisotropic part of the curve potential energy density in terms of the tangent vectors $\boldsymbol{t}$ and $\boldsymbol{T}$, respectively.

7. Conclusion

Motivated by the observation that in many cases the boundary of a continuum body displays different mechanical properties as compared to its bulk, this contribution systematically explored deformational and configurational mechanics incorporating separate boundary potentials. Thereby the (localized) force balances (in the bulk and) at surfaces, curves and points have been derived variationally, i.e. within a conservative setting, for the deformational and the configurational case. In order to pursue an unified approach the relevant curve quantities have thereby been treated in a tensor rather than the common vector representation. The key philosophy of this contribution is to define configurational forces as capturing energetic changes that go along with material variations (configurational changes) when deriving the configurational setting. The main thrust of this contribution is, thereby, to highlight the striking duality of the (localized) format of the force balances (in the bulk and) at surfaces, curves and points within deformational and configurational mechanics. As an interesting result it turns out that for perfect, i.e. defect free surfaces and curves the tangential part of the corresponding (localized) force balances can be cast into four different formats by performing either the relevant Piola transformations or pull back/push forward operations. The remaining non-trivial configurational forces acting on: (i) surfaces are scalar valued and normal to the surface; (ii) curves are vector valued and perpendicular to the curve; (ii) on points are vector valued. Finally, the relevant equations pertaining to (the bulk,) surfaces, curves and points have been put into a format that emphasizes, as much as possible, the similarities (and differences) between these different geometric objects of dimension (3), 2, 1, 0, respectively.

References

Abeyaratne, R., Knowles, J.K., 1990. On the driving traction acting on a surface of strain discontinuity in a continuum. J. Mech. Phys. Solids 38, 345–360.

Angenent, S., Gurtin, M.E., 1989. Multiphase thermomechanics with interfacial structure. Part 1. Arch. Rational Mech. Anal. 108, 323–391.

Capriz, G., Mariano, P.M., 2004. Balances at a junction among coherent interfaces in materials with substructure. In: Capriz, G., Mariano, P.M. (Eds.), Advances in Multifield Theories for Continua with Substructure. Birkhäuser, Boston, pp. 243–263.

Dingreville, R., Qu, J., Cherkaoui, M., 2005. Surface free energy and its effect on the elastic behavior of nano-sized particles, wires and films. J. Mech. Phys. Solids. 53, 1827–1854.

Eshelby, J.D., 1951. The force on an elastic singularity. Phil. Trans. Roy. Soc. London A 244, 87–112.

Gasser, T.C., Holzapfel, G.A., 2003. Geometrically non-linear and consistently linearized embedded strong discontinuity models for 3d problems with an application to the dissection analysis of soft biological tissues. Comput. Methods Appl. Mech. Eng. 192, 5059–5098.

Gurtin, M.E., 1988. Multiphase thermomechanics with interfacial structure Part 1. Arch. Rational Mech. Anal. 104, 185–221.

Gurtin, M.E., 1993. The dynamics of solid–solid phase transitions Part 1. Arch. Rational Mech. Anal. 123, 305–335.

Gurtin, M.E., 1995. On the nature of configurational forces. Arch. Rational Mech. Anal. 131, 67–100.

Gurtin, M.E., 2000. Configurational Forces as Basic Concepts of Continuum Physics. Springer, New York.

Gurtin, M.E., Murdoch, A., 1975. A continuum theory of elastic material surfaces. Arch. Rational Mech. Anal. 57, 291–323.

Gurtin, M.E., Struthers, A., 1990. Multiphase thermomechanics with interfacial structure. Part 3. Arch. Rational Mech. Anal. 112, 97–160.

Kienzler, R., Herrmann, G., 2000. Mechanics in Material Space. Springer, Berlin.

Leo, P., Sekerka, R.F., 1989. The effect of surface stress on crystal-melt and crystal-crystal equilibrium. Act. Metall. 37, 3119–3138.

Mariano, P.M., 2000. Configurational forces in continua with microstruture. ZAMP 51, 752–791.

Mariano, P.M., 2001. Coherent interfaces with junctions in continua with microstructures. Int. J. Solids Struct. 38, 1243–1267.

Mariano, P.M., 2002. Multifield theories in mechanics of solids. Adv. Appl. Mech. 38, 1–94.

Maugin, G.A., 1993. Material Inhomogeneities in Elasticity. Chapman & Hall, London.

Maugin, G.A., 1995. Material forces: concepts and applications. Appl. Mech. Rev. 48, 213–245.

Maugin, G.A., 1997. Thermomechanics of inhomogeneous–heterogeneous systems: application to the irreversible progress of two- and three-dimensional defects. ARI 50, 41–56.

Maugin, G.A., 1998a. On shock waves and phase-transition fronts in continua. ARI 50, 141–150.

Maugin, G.A., 1998b. Thermomechanics of forces driving singular pointsets. Arch. Mech. 50, 509–519.

Maugin, G.A., 1999. On the universality of the thermomechanics of forces driving singular sets. Arch. Appl. Mech. 69, 1–15.

Maugin, G.A., Trimarco, C., 1992. Pseudomomentum and material forces in nonlinear elasticity: variational formulations and application to brittle fracture. Acta Mech. 94, 1–28.

Maugin, G.A., Trimarco, C., 1995. The dynamics of configurational forces at phase-transition fronts. Meccanica 30, 605–619.

Šilhavý, M., 1997. The Mechanics and Thermodynamics of Continuous Media. Springer, Berlin.

Simha, N.K., Bhattacharya, K., 1998. Kinetics of phase boundaries with edges and junctions. J. Mech. Phys. Solids 46, 2323–2359.

Simha, N.K., Bhattacharya, K., 2000. Kinetics of phase boundaries with edges and junctions in a three-dimensional multi-phase body. J. Mech. Phys. Solids 48, 2619–2641.

Steinmann, P., 2002a. On spatial and material settings of hyper-elastodynamics. Acta Mech. 156, 193–218.

Steinmann, P., 2002b. On spatial and material settings of thermo-hyperelastodynamics. J. Elasticity 66, 109–157.

Steinmann, P., 2002c. On spatial and material settings of hyperelastostatic crystal defects. J. Mech. Phys. Solids 50, 1743–1766.